

## CHAPTER 4

# SENSORS FOR MAP-BASED POSITIONING

Most sensors used for the purpose of map building involve some kind of distance measurement. There are three basically different approaches to measuring range:

- Sensors based on measuring the *time of flight* (TOF) of a pulse of emitted energy traveling to a reflecting object, then echoing back to a receiver.
- The *phase-shift measurement* (or *phase-detection*) ranging technique involves continuous wave transmission as opposed to the short pulsed outputs used in TOF systems.
- Sensors based on frequency-modulated (FM) radar. This technique is somewhat related to the (amplitude-modulated) phase-shift measurement technique.

### 4.1 Time-of-Flight Range Sensors

Many of today's range sensors use the *time-of-flight* (TOF) method. The measured pulses typically come from an ultrasonic, RF, or optical energy source. Therefore, the relevant parameters involved in range calculation are the speed of sound in air (roughly 0.3 m/ms — 1 ft/ms), and the speed of light (0.3 m/ns — 1 ft/ns). Using elementary physics, distance is determined by multiplying the velocity of the energy wave by the time required to travel the round-trip distance:

$$d = v t \tag{4.1}$$

where

- $d$  = round-trip distance
- $v$  = speed of propagation
- $t$  = elapsed time.

The measured time is representative of traveling twice the separation distance (i.e., out and back) and must therefore be reduced by half to result in actual range to the target.

The advantages of TOF systems arise from the direct nature of their straight-line active sensing. The returned signal follows essentially the same path back to a receiver located coaxially with or in close proximity to the transmitter. In fact, it is possible in some cases for the transmitting and receiving transducers to be the same device. The absolute range to an observed point is directly available as output with no complicated analysis required, and the technique is not based on any assumptions concerning the planar properties or orientation of the target surface. The *missing parts* problem seen in triangulation does not arise because minimal or no offset distance between transducers is needed. Furthermore, TOF sensors maintain range accuracy in a linear fashion as long as reliable echo detection is sustained, while triangulation schemes suffer diminishing accuracy as distance to the target increases.

Potential error sources for TOF systems include the following:

- Variations in the speed of propagation, particularly in the case of acoustical systems.
- Uncertainties in determining the exact time of arrival of the reflected pulse.

- Inaccuracies in the timing circuitry used to measure the round-trip time of flight.
- Interaction of the incident wave with the target surface.

Each of these areas will be briefly addressed below, and discussed later in more detail.

**a. Propagation Speed** For mobile robotics applications, changes in the propagation speed of electromagnetic energy are for the most part inconsequential and can basically be ignored, with the exception of satellite-based position-location systems as presented in Chapter 3. This is not the case, however, for acoustically based systems, where the speed of sound is markedly influenced by temperature changes, and to a lesser extent by humidity. (The speed of sound is actually proportional to the square root of temperature in degrees Rankine.) An ambient temperature shift of just 30° F can cause a 0.3 meter (1 ft) error at a measured distance of 10 meters (35 ft) [Everett, 1985].

**b. Detection Uncertainties** So-called *time-walk errors* are caused by the wide dynamic range in returned signal strength due to varying reflectivities of target surfaces. These differences in returned signal intensity influence the rise time of the detected pulse, and in the case of fixed-threshold detection will cause the more reflective targets to appear closer. For this reason, *constant* fraction timing discriminators are typically employed to establish the detector threshold at some specified fraction of the peak value of the received pulse [Vuylsteke et al., 1990].

**c. Timing Considerations** Due to the relatively slow speed of sound in air, compared to light, acoustically based systems face milder timing demands than their light-based counterparts and as a result are less expensive. Conversely, the propagation speed of electromagnetic energy can place severe requirements on associated control and measurement circuitry in optical or RF implementations. As a result, TOF sensors based on the speed of light require sub-nanosecond timing circuitry to measure distances with a resolution of about a foot [Koenigsburg, 1982]. More specifically, a desired resolution of 1 millimeter requires a timing accuracy of 3 picoseconds ( $3 \times 10^{-12}$  s) [Vuylsteke et al., 1990]. This capability is somewhat expensive to realize and may not be cost effective for certain applications, particularly at close range where high accuracies are required.

**d. Surface Interaction** When light, sound, or radio waves strike an object, any detected echo represents only a small portion of the original signal. The remaining energy reflects in scattered directions and can be absorbed by or pass through the target, depending on surface characteristics and the angle of incidence of the beam. Instances where no return signal is received at all can occur because of specular reflection at the object's surface, especially in the ultrasonic region of the energy spectrum. If the transmission source approach angle meets or exceeds a certain critical value, the reflected energy will be deflected outside of the sensing envelope of the receiver. In cluttered environments soundwaves can reflect from (multiple) objects and can then be received by other sensors. This phenomenon is known as crosstalk (see Figure 4.1). To compensate, repeated measurements are often averaged to bring the signal-to-noise ratio within acceptable levels, but at the expense of additional time required to determine a single range value. Borenstein and Koren [1995] proposed a method that allows individual sensors to detect and reject crosstalk.

Using this method much faster firing rates — under 100 ms for a complete scan with 12 sonars — are feasible.

#### 4.1.1 Ultrasonic TOF Systems

Ultrasonic TOF ranging is today the most common technique employed on indoor mobile robotics systems, primarily due to the ready availability of low-cost systems and their ease of interface. Over the past decade, much research has been conducted investigating applicability in such areas as world modeling and collision avoidance, position estimation, and motion detection. Several researchers have more recently begun to assess the effectiveness of ultrasonic sensors in exterior settings [Pletta et al., 1992; Langer and Thorpe, 1992; Pin and Watanabe, 1993; Hammond, 1994]. In the automotive industry, BMW now incorporates four piezoceramic transducers (sealed in a membrane for environmental protection) on both front and rear bumpers in its Park Distance Control system [Siuru, 1994]. A detailed discussion of ultrasonic sensors and their characteristics with regard to indoor mobile robot applications is given in [Jörg, 1994].

Two of the most popular commercially available ultrasonic ranging systems will be reviewed in the following sections.

##### 4.1.1.1 Massa Products Ultrasonic Ranging Module Subsystems

Massa Products Corporation, Hingham, MA, offers a full line of ultrasonic ranging subsystems with maximum detection ranges from 0.6 to 9.1 meters (2 to 30 ft) [MASSA]. The *E-201B series* sonar operates in the bistatic mode with separate transmit and receive transducers, either side by side for echo ranging or as an opposed pair for unambiguous distance measurement between two uniquely defined points. This latter configuration is sometimes used in ultrasonic position location systems and provides twice the effective operating range with respect to that advertised for conventional echo ranging. The *E-220B series* (see Figure 4.2) is designed for monostatic (single transducer) operation but is otherwise functionally identical to the *E-201B*. Either version can be externally triggered on command, or internally triggered by a free-running oscillator at a repetition rate determined by an external resistor (see Figure 4.3).

Selected specifications for the four operating frequencies available in the *E-220B series* are listed in Table 4.1 below. A removable focusing horn is provided for the 26- and 40-kHz models that decreases the effective beamwidth (when installed) from 35 to 15 degrees. The horn must be in place to achieve the maximum listed range.

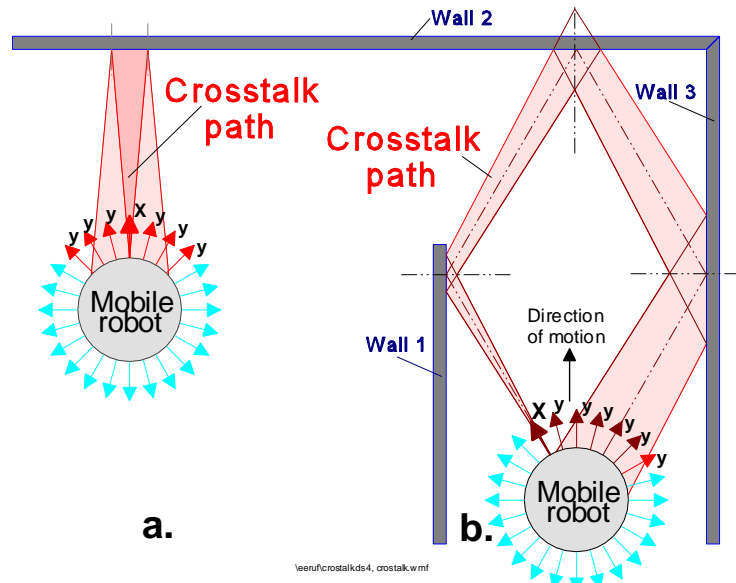


**Figure 4.1:** Crosstalk is a phenomenon in which one sonar picks up the echo from another. One can distinguish between a. direct crosstalk and b. indirect crosstalk.

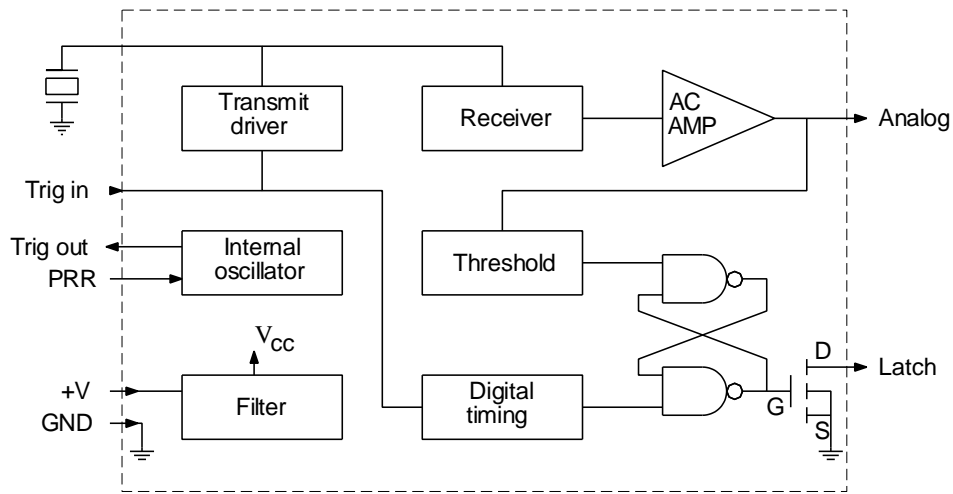


**Figure 4.2:** The single-transducer Massa *E-220B-series* ultrasonic ranging module can be internally or externally triggered, and offers both analog and digital outputs. (Courtesy of Massa Products Corp.)

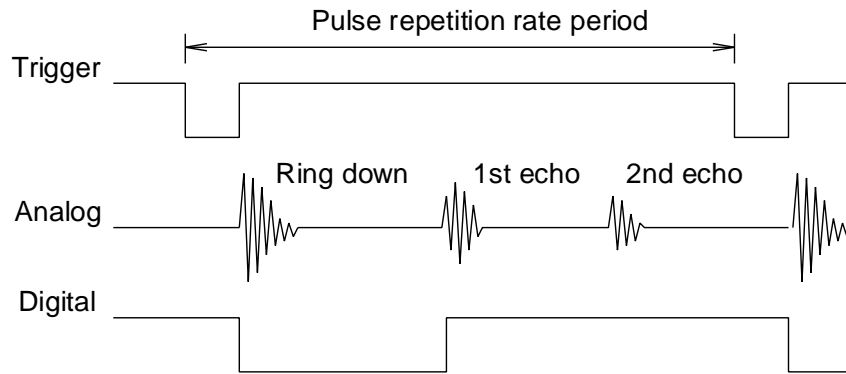


**Figure 4.3:** Timing diagram for the *E-220B series* ranging module showing analog and digital output signals in relationship to the trigger input. (Courtesy of Massa Products Corp.)

**Table 4.1:** Specifications for the monostatic E-220B Ultrasonic Ranging Module Subsystems. The E-201 series is a bistatic configuration with very similar specifications. (Courtesy of Massa Products Corp.)

Parameter	E-220B/215	E-220B/150	E-220B/40	E-220B/26	Units
Range	10 - 61	20 - 152	61 - 610	61 - 914	cm
	4 - 24	8 - 60	24 - 240	24 - 360	in
Beamwidth	10	10	35 (15)	35 (15)	°
Frequency	215	150	40	26	kHz
Max rep rate	150	100	25	20	Hz
Resolution	0.076	0.1	0.76	1	cm
	0.03	0.04	0.3	0.4	in
Power	8 - 15	8 - 15	8 - 15	8 - 15	VDC
Weight	4 - 8	4 - 8	4 - 8	4 - 8	oz

#### 4.1.1.2 Polaroid Ultrasonic Ranging Modules

The Polaroid ranging module is an active TOF device developed for automatic camera focusing, which determines the range to target by measuring elapsed time between the transmission of an ultrasonic waveform and the detected echo [Biber et al., 1987, POLAROID]. This system is the most widely found in mobile robotics literature [Koenigsburg, 1982; Moravec and Elfes, 1985; Everett, 1985; Kim, 1986; Moravec, 1988; Elfes, 1989; Arkin, 1989; Borenstein and Koren, 1990; 1991a; 1991b; 1995; Borenstein et al., 1995], and is representative of the general characteristics of such ranging devices.

The most basic configuration consists of two fundamental components: 1) the ultrasonic transducer, and 2) the ranging module electronics. Polaroid offers OEM kits with two transducers and two ranging module circuit boards for less than \$100 (see Figure 4.4).

A choice of transducer types is now available. In the original instrument-grade electrostatic version, a very thin metal diaphragm mounted on a machined backplate formed a capacitive transducer as illustrated in Figure 4.5 [POLAROID, 1991]. The system operates in the monostatic transceiver mode so that only a single transducer is necessary to acquire range data. A smaller diameter electrostatic transducer (*7000-series*) has also been made available, developed for the Polaroid *Spectra* camera [POLAROID, 1987]. A more rugged piezoelectric (*9000-series*) environmental transducer for applications in severe environmental conditions including vibration is able to meet or exceed the SAE J1455 January 1988 specification for heavy-duty trucks. Table 4.2 lists the technical specifications for the different Polaroid transducers.

The original Polaroid ranging module functioned by transmitting a *chirp* of four discrete fre-

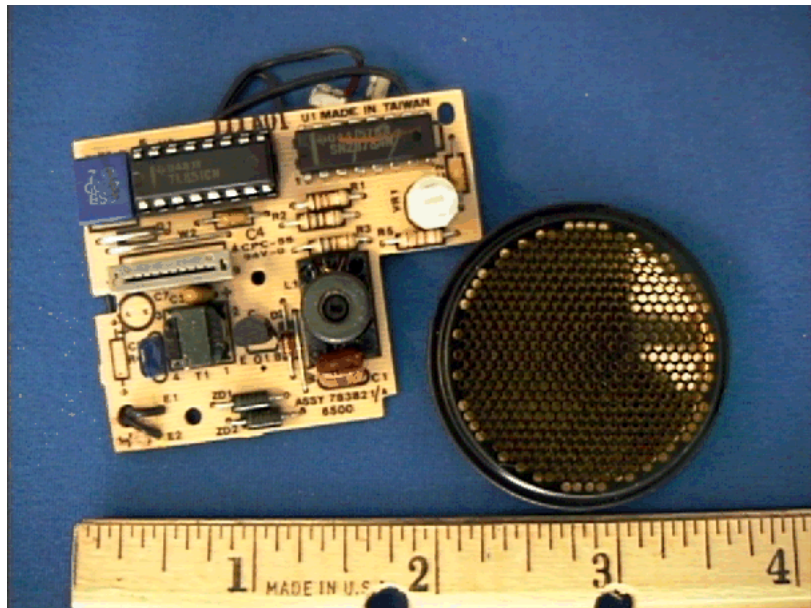


**Figure 4.4:** The Polaroid OEM kit included the transducer and a small electronics interface board.

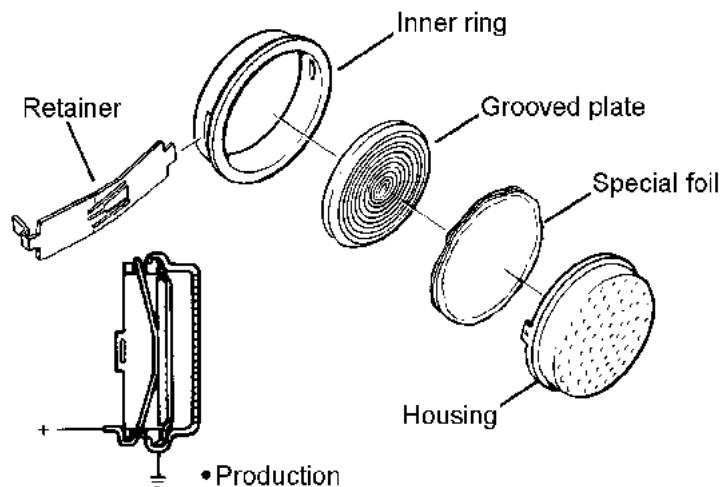


**Figure 4.5:** The Polaroid instrument grade electrostatic transducer consists of a gold-plated plastic foil stretched across a machined backplate. (Reproduced with permission from Polaroid [1991].)

quencies at about of 50 kHz. The SN28827 module was later developed with reduced parts count, lower power consumption, and simplified computer interface requirements. This second-generation board transmits only a single frequency at 49.1 kHz. A third-generation board (*6500 series*) introduced in 1990 provided yet a further reduction in interface circuitry, with the ability to detect and report multiple echoes [Polaroid, 1990]. An *Ultrasonic Ranging Developer's Kit* based on the Intel 80C196 microprocessor is now available for use with the *6500 series* ranging module that allows software control of transmit frequency, pulse width, blanking time, amplifier gain, and maximum range [Polaroid, 1993].

The range of the Polaroid system runs from about 41 centimeters to 10.5 meters (1.33 ft to 35 ft). However, using custom circuitry suggested in [POLAROID, 1991] the minimum range can be reduced reliably to about 20 centimeters (8 in) [Borenstein et al., 1995]. The beam dispersion angle is approximately 30 degrees. A typical operating cycle is as follows.

1. The control circuitry fires the transducer and waits for indication that transmission has begun.
2. The receiver is blanked for a short period of time to prevent false detection due to ringing from residual transmit signals in the transducer.
3. The received signals are amplified with increased gain over time to compensate for the decrease in sound intensity with distance.
4. Returning echoes that exceed a fixed threshold value are recorded and the associated distances calculated from elapsed time.

**Table 4.2:** Specifications for the various Polaroid ultrasonic ranging modules. (Courtesy of Polaroid.)

Parameter	Original	SN28827	6500	Units
Maximum range	10.5	10.5	10.5	m
	35	35	35	ft
Minimum range*	25	20	20	cm
	10.5	6	6	in
Number of pulses	56	16	16	
Blanking time	1.6	2.38	2.38	ms
Resolution	1	2	1	%
Gain steps	16	12	12	
Multiple echo	no	yes	yes	
Programmable frequency	no	no	yes	
Power	4.7 - 6.8	4.7 - 6.8	4.7 - 6.8	V
	200	100	100	mA

\* with custom electronics (see [Borenstein et al., 1995].)

Figure 4.6 [Polaroid, 1990] illustrates the operation of the sensor in a timing diagram. In the *single-echo* mode of operation for the *6500-series* module, the *blank* (BLNK) and *blank-inhibit* (BINH) lines are held low as the *initiate* (INIT) line goes high to trigger the outgoing pulse train. The *internal blanking* (BLANKING) signal automatically goes high for 2.38 milliseconds to prevent transducer ringing from being misinterpreted as a returned echo. Once a valid return is received, the echo (ECHO) output will latch high until reset by a high-to-low transition on INIT.

For multiple-echo processing, the *blanking* (BLNK) input must be toggled high for at least 0.44 milliseconds after detection of the first return signal to reset the *echo* output for the next return.

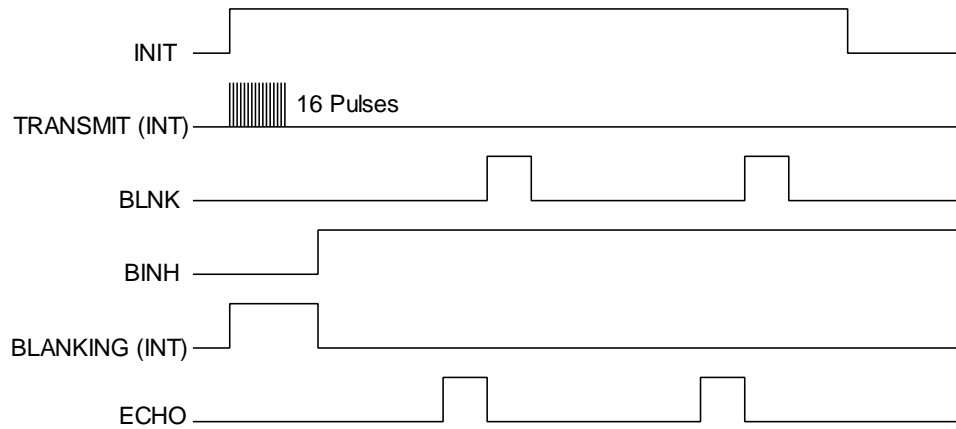


**Figure 4.6:** Timing diagram for the 6500-Series Sonar Ranging Module executing a multiple-echo-mode cycle with blanking input. (Courtesy of Polaroid Corp.)

### 4.1.2 Laser-Based TOF Systems

Laser-based TOF ranging systems, also known as *laser radar* or *lidar*, first appeared in work performed at the Jet Propulsion Laboratory, Pasadena, CA, in the 1970s [Lewis and Johnson, 1977]. Laser energy is emitted in a rapid sequence of short bursts aimed directly at the object being ranged. The time required for a given pulse to reflect off the object and return is measured and used to calculate distance to the target based on the speed of light. Accuracies for early sensors of this type could approach a few centimeters over the range of 1 to 5 meters (3.3 to 16.4 ft) [NASA, 1977; Depkovich and Wolfe, 1984].

#### 4.1.2.1 Schwartz Electro-Optics Laser Rangefinders

Schwartz Electro-Optics, Inc. (SEO), Orlando, FL, produces a number of laser TOF rangefinding systems employing an innovative time-to-amplitude-conversion scheme to overcome the sub-nanosecond timing requirements necessitated by the speed of light. As the laser fires, a precision capacitor begins discharging from a known set point at a constant rate. An analog-to-digital conversion is performed on the sampled capacitor voltage at the precise instant a return signal is detected, whereupon the resulting digital representation is converted to range using a look-up table.

#### SEO LRF-200 OEM Laser Rangefinders

The *LRF-200 OEM Laser Rangefinder* shown in Figure 4.7 features compact size, high-speed processing, and the ability to acquire range information from most surfaces (i.e., minimum 10-percent Lambertian reflectivity) out to a maximum of 100 meters (328 ft). The basic system uses a pulsed InGaAs laser diode in conjunction with an avalanche photodiode detector, and is available with both analog and digital (RS-232) outputs. Table 4.3 lists general specifications for the sensor's performance [SEO, 1995a].



**Figure 4.7:** The LRF-200 OEM Laser Rangefinder. (Courtesy of Schwartz Electro-Optics, Inc.)

Another adaptation of the LRF-200 involved the addition of a mechanical single-DOF beam scanning capability. Originally developed for use in submunition sensor research, the *Scanning Laser Rangefinder* is currently installed on board a remotely piloted vehicle. For this application, the sensor is positioned so the forward motion of the RPV is perpendicular to the vertical scan plane, since three-dimensional target profiles are required [SEO, 1991b]. In a second application, the *Scanning Laser Rangefinder* was used by the Field Robotics Center at Carnegie Mellon University as a terrain mapping sensor on their unmanned autonomous vehicles.

**Table 4.3:** Selected specifications for the LRF 200 OEM Laser Rangefinder. (Courtesy of Schwartz Electro-Optics, Inc.)

Parameter	Value	Units
Range (non-cooperative target)	1 to 100	m
	3.3-328	ft
Accuracy	±30	cm
	±12	in
Range jitter	±12	cm
	±4.7	in
Wavelength	902	nm
Diameter	89	mm
	3.5	in
Length	178	mm
	7	in
Weight	1	kg
	2.2	lb
Power	8 to 24	VDC
	5	W

**Table 4.4:** Selected specifications for the SEO Scanning Laser Rangefinder. (Courtesy of Schwartz Electro-Optics, Inc.)

Parameter	Value	Units
Range	1-100	m
	3.3-330	ft
Accuracy	±30	cm
	±12	in
Scan angle	±30	°
Scan rate	24.5- 30.3	kHz
Samples per scan	175	
Wavelength	920	nm
Diameter	127	mm
	5	in
Length	444	mm
	17.5	in
Weight	5.4	kg
	11.8	lb
Power	8-25	VDC



### SEO Scanning Helicopter Interference Envelope Laser Detector (SHIELD)

This system was developed for the U.S. Army [SEO, 1995b] as an onboard pilot alert to the presence of surrounding obstructions in a 60-meter radius hemispherical envelope below the helicopter. A high-pulse-repetition-rate GaAs eye-safe diode emitter shares a common aperture with a sensitive avalanche photodiode detector. The transmit and return beams are reflected from a motor-driven prism rotating at 18 rps (see Figure 4.9). Range measurements are correlated with the azimuth angle using an optical encoder. Detected obstacles are displayed on a 5.5-inch color monitor. Table 4.5 lists the key specifications of the *SHIELD*.

**Table 4.5:** Selected specifications for the *Scanning Helicopter Interference Envelope Laser Detector (SHIELD)*. (Courtesy of Schwartz Electro-Optics, Inc.)

Parameter	Value	Units
Maximum range (hemispherical envelope)	>60 m >200 ft	
Accuracy	<30 cm 1 ft	
Wavelength	905 nm	
Scan angle	360 °	
Scan rate	18 Hz	
Length	300 mm 11.75 in	
Weight	15 lb	
Power	18 VDC <5 A	

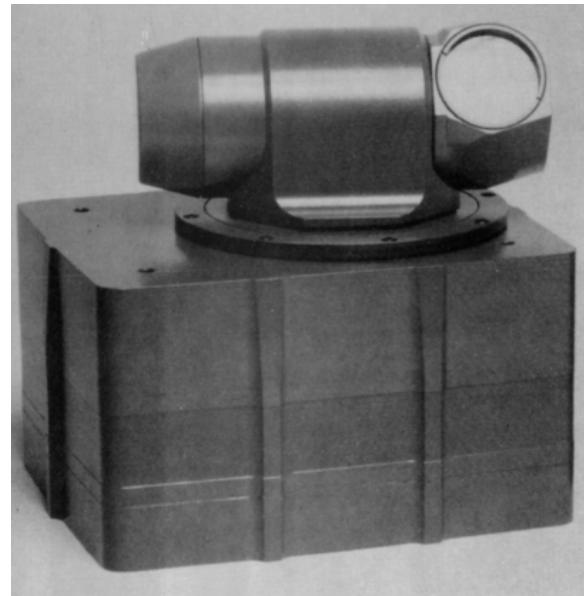


**Figure 4.8:** The *Scanning Helicopter Interference Envelope Laser Detector (SHIELD)*. (Courtesy of Schwartz Electro-Optics, Inc.)

### SEO TreeSense

The *TreeSense* system was developed by SEO for automating the selective application of pesticides to orange trees, where the goal was to enable individual spray nozzles only when a tree was detected within their associated field of coverage. The sensing subsystem (see Figure 4.9) consists of a horizontally oriented unit mounted on the back of an agricultural vehicle, suitably equipped with a rotating mirror arrangement that scans the beam in a vertical plane orthogonal to the direction of travel. The scan rate is controllable up to 40 rps (35 rps typical). The ranging subsystem is gated on and off twice during each revolution to illuminate two 90-degree fan-shaped sectors to a maximum range of 7.6 meters (25 ft) either side of the vehicle as shown in Figure 4.10. The existing hardware is theoretically capable of ranging to 9 meters (30 ft) using a PIN photodiode and can be extended further through an upgrade option that incorporates an avalanche photodiode detector.

The *TreeSense* system is hard-wired to a valve manifold to enable/disable a vertical array of nozzles for the spraying of insecticides, but analog as well as digital (RS-232) output can easily be made available for other applications. The system is housed in a rugged aluminum enclosure with a total weight of only 2.2 kilograms (5 lb). Power requirements are 12 W at 12 VDC. Further details on the system are contained in Table 4.6.

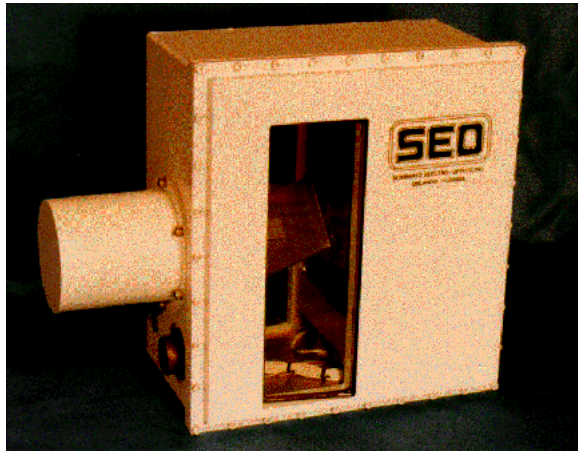


**Figure 4.9:** The SEO *TreeSense*. (Courtesy of Schwartz Electro-Optics, Inc.)

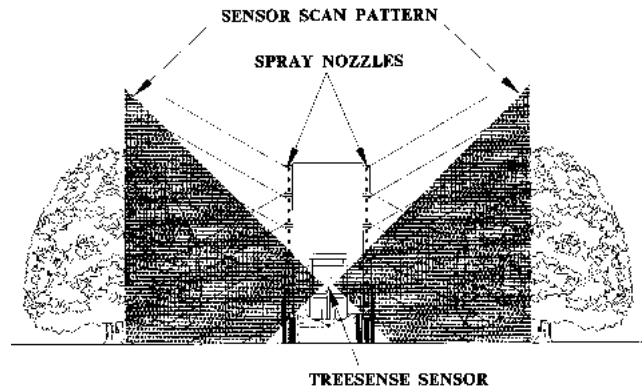


**Figure 4.10:** Scanning pattern of the SEO *TreeSense* system. (Courtesy of Schwartz Electro-Optics, Inc.)

**SEO *AutoSense***

The *AutoSense I* system was developed by SEO under a Department of Transportation Small Business Innovative Research (SBIR) effort as a replacement for buried inductive loops for traffic signal control. (Inductive loops don't always sense motorcyclists and some of the smaller cars with fiberglass or plastic body panels, and replacement or maintenance can be expensive as well as disruptive to traffic flow.) The system is configured to look down at about a 30-degree angle on moving vehicles in a traffic lane as illustrated in Figure 4.12.

*AutoSense I* uses a PIN photo-diode detector and a pulsed (8 ns) InGaAs near-infrared laser-diode source with peak power of 50 W. The laser output is directed by a beam splitter into a pair of cylindrical lenses to generate two fan-shaped beams 10 degrees apart in elevation for improved target detection. (The original prototype projected only a single spot of light, but ran into problems due to target absorption and specular reflection.) As an added benefit, the use of two separate beams makes it possible to calculate the speed of moving vehicles to an accuracy of 1.6 km/h (1 mph). In addition, a two-dimensional image (i.e., length and

**Table 4.6:** Selected specifications for the *TreeSense* system. (Courtesy of Schwartz Electro-Optics, Inc.)

Parameter	Value	Units
Maximum range	9 m 30 ft	
Accuracy (in % of measured range)	1	%
Wavelength	902	nm
Pulse repetition frequency	15	KHz
Scan rate	29.3	rps
Length	229 mm 9 in	
Width	229 mm 9 in	
Height	115 mm 4.5 in	
Weight	5	lbs
Power	12 V 12 W	

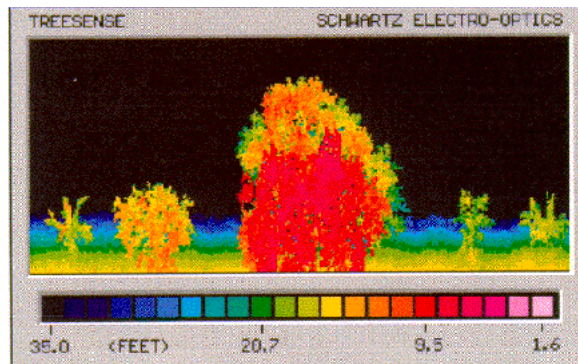


**Figure 4.11:** Color-coded range image created by the SEO *TreeSense* system. (Courtesy of Schwartz Electro-Optics, Inc.)

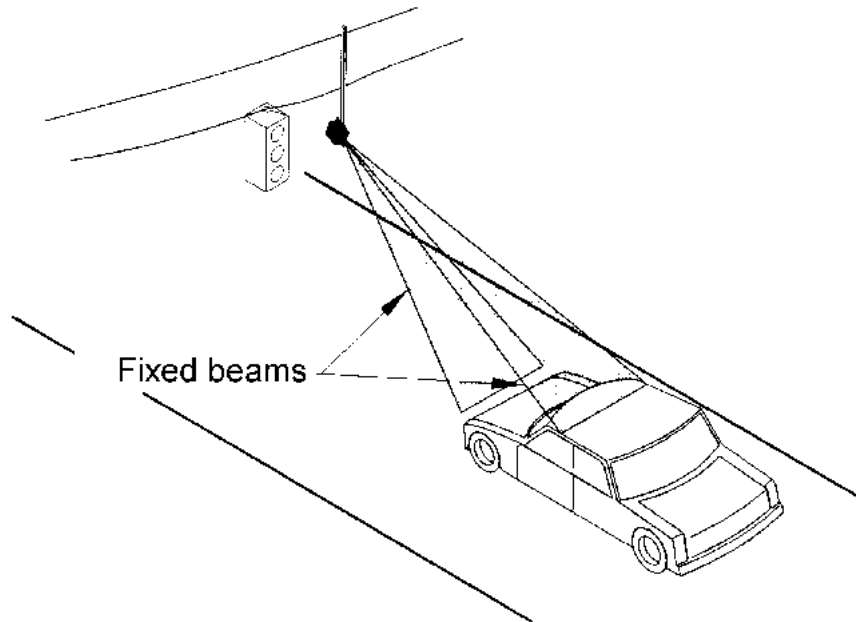


**Figure 4.12:** Two fan-shaped beams look down on moving vehicles for improved target detection. (Courtesy of Schwartz Electro-Optics, Inc.)

width) is formed of each vehicle as it passes through the sensor's field of view, opening the door for numerous vehicle classification applications under the Intelligent Vehicle Highway Systems concept.

*AutoSense II* is an improved second-generation unit (see Figure 4.13) that uses an avalanche photodiode detector instead of the PIN photodiode for greater sensitivity, and a multi-faceted rotating mirror with alternating pitches on adjacent facets to create the two beams. Each beam is scanned across the traffic lane 720 times per second, with 15 range measurements made per scan. This azimuthal scanning action generates a precise three-dimensional profile to better facilitate vehicle classification in automated toll booth applications. An abbreviated system block diagram is depicted in Figure 4.14.



**Figure 4.13:** The *AutoSense II* is SEO's active-infrared overhead vehicle imaging sensor. (Courtesy of Schwartz Electro-Optics, Inc.)

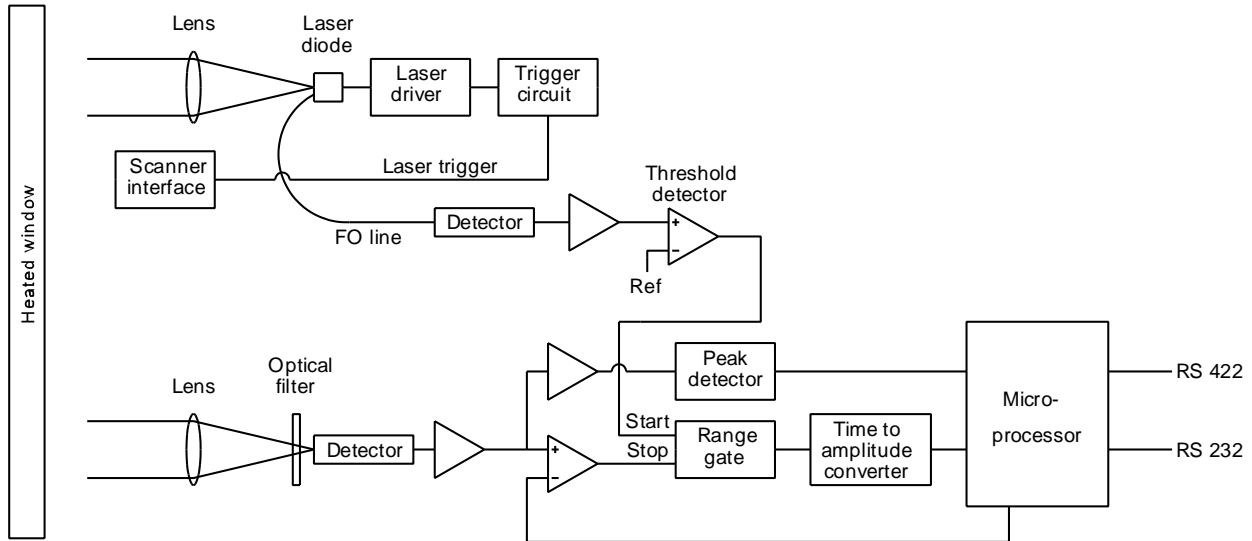


**Figure 4.14:** Simplified block diagram of the *AutoSense II* time-of-flight 3-D ranging system. (Courtesy of Schwartz Electro-Optics, Inc.)

Intensity information from the reflected signal is used to correct the “time-walk” error in threshold detection resulting from varying target reflectivities, for an improved range accuracy of 7.6 cm (3 in) over a 1.5 to 15 m (5 to 50 ft) field of regard. The scan resolution is 1 degree, and vehicle velocity can be calculated with an accuracy of 3.2 km/h (2 mph) at speeds up to 96 km/h (60 mph). A typical scan image created with the *Autosense II* is shown in Figure 4.15.

A third-generation *AutoSense III* is now under development for an application in Canada that requires 3-dimensional vehicle profile generation at speeds up to 160 km/h (100 mph). Selected specifications for the *AutoSense II* package are provided in Table 4.7.

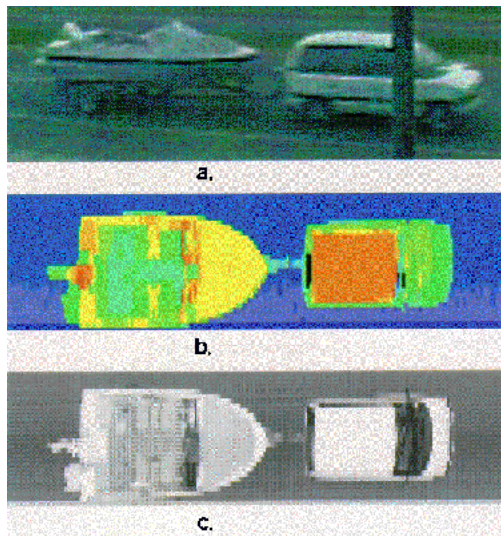


**Figure 4.15:** Output sample from a scan with the *AutoSense II*.  
 a. Actual vehicle with trailer (photographed with a conventional camera).  
 b. Color-coded range information.  
 c. Intensity image.  
 (Courtesy of Schwartz Electro-Optics, Inc.)

**Table 4.7:** Selected specifications for the *AutoSense II* ranging system. (Courtesy of Schwartz Electro-Optics, Inc.)

Parameter	Value	Units
Range	0.61-1.50	m
		2-50
Accuracy	7.5	cm
		3
Wavelength	904	nm
Pulse repetition rate	86.4	kHz
Scan rate	720	scans/s/scanline
Range readings per scan	30	
Weight	11.4	kg
		25
Power	115	VAC
		75

#### 4.1.2.2 RIEGL Laser Measurement Systems

RIEGL Laser Measurement Systems, Horn, Austria, offers a number of commercial products (i.e., laser binoculars, surveying systems, “speed guns,” level sensors, profile measurement systems, and tracking laser scanners) employing short-pulse TOF laser ranging. Typical applications include lidar altimeters, vehicle speed measurement for law enforcement, collision avoidance for cranes and vehicles, and level sensing in silos. All RIEGL products are distributed in the United States by RIEGEL USA, Orlando, FL.

##### **LD90-3 Laser Rangefinder**

The RIEGL *LD90-3 series* laser rangefinder (see Figure 4.16) employs a near-infrared laser diode source and a photodiode detector to perform TOF ranging out to 500 meters (1,640 ft) with diffuse surfaces, and to over 1,000 meters (3,281 ft) in the case of co-operative targets. Round-trip propagation time is precisely measured by a quartz-stabilized clock and converted to measured distance by an internal microprocessor using one of two available algorithms. The clutter suppression algorithm incorporates a combination of range measurement averaging and noise rejection techniques to filter out backscatter from airborne particles, and is therefore useful when operating under conditions of poor visibility [Riegl, 1994]. The *standard measurement* algorithm, on the other hand, provides rapid range measurements without regard for noise suppression, and can subsequently deliver a higher update rate under more favorable environmental conditions. Worst-case range measurement accuracy is  $\pm 5$  centimeters ( $\pm 2$  in), with typical values of around  $\pm 2$  centimeters ( $\pm 0.8$  in). See Table 4.8 for a complete listing of the LD90-3's features.

The pulsed near-infrared laser is Class-1 eye safe under all operating conditions. A nominal beam divergence of 0.1 degrees (2 mrad) for the LD90-3100 unit (see Tab. 4.9 below) produces a 20 centimeter (8 in) footprint of illumination at 100 meters (328 ft) [Riegl, 1994]. The complete system is housed in a small light-weight metal enclosure weighing only 1.5 kilograms (3.3 lb), and draws 10 W at 11 to 18 VDC. The standard output format is serial RS-232 at programmable data



**Figure 4.16:** The RIEGL *LD90-3 series* laser rangefinder. (Courtesy of Riegl USA.)

rates up to 19.2 kilobits per second, but RS-422 as well as analog options (0 to 10 VDC and 4 to 20 mA current-loop) are available upon request.

Table 4.8: Selected specifications for the RIEGL LD90-3 series laser rangefinder. (Courtesy of RIEGL Laser Measurement Systems.)

Parameter		LD90-3100	LD90-3300	Units
Maximum range	(diffuse)	150	400	m
		492	1,312	ft
	(cooperative)	>1000	>1000	m
		>3,280	>3,280	ft
Minimum range		1	3-5	m
Accuracy	(distance)	2	5	cm
		$\frac{3}{4}$	2	in
	(velocity)	0.3	0.5	m/s
Beam divergence		2	2.8	mrad
Output	(digital)	RS-232, -422	RS-232, -422	
	(analog)	0-10	0-10	VDC
Power		11-18	11-18	VDC
		10	10	W
Size		22×13×7.6	22×13×7.6	cm
		8.7×5.1×3	8.7×5.1×3	in
Weight		3.3	3.3	lb

### Scanning Laser Rangefinders

The LRS90-3 Laser Radar Scanner is an adaptation of the basic LD90-3 electronics, fiber-optically coupled to a remote scanner unit as shown in Figure 4.17. The scanner package contains no internal electronics and is thus very robust under demanding operating conditions typical of industrial or robotics scenarios. The motorized scanning head pans the beam back and forth in the horizontal plane at a 10-Hz rate, resulting in 20 data-gathering sweeps per second. Beam divergence is 0.3 degrees (5 mrad) with the option of expanding in the vertical direction if desired up to 2 degrees.

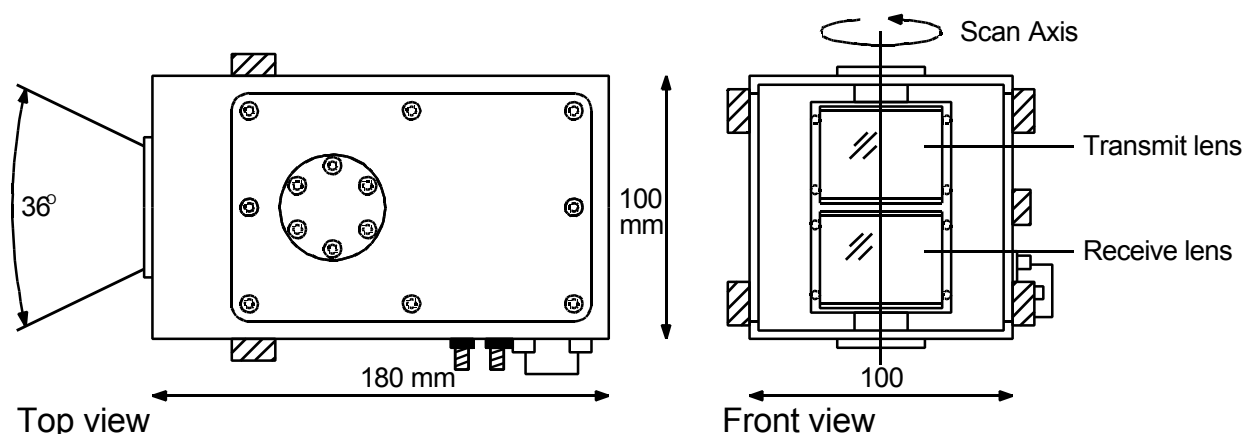


Figure 4.17: The LRS90-3 Laser Radar Scanner consists of an electronics unit (not shown) connected via a duplex fiber-optic cable to the remote scanner unit depicted above. (Courtesy of RIEGL USA.)

The *LSS390 Laser Scanning System* is very similar to the *LRS90-3*, but scans a more narrow field of view ( $10^\circ$ ) with a faster update rate (2000 Hz) and a more tightly focused beam. Range accuracy is 10 centimeters (4 in) typically and 20 centimeters (8 in) worst case. The *LSS390* unit is available with an RS-422 digital output (19.2 kbs standard, 150 kbs optional) or a 20 bit parallel TTL interface.

**Table 4.9:** Typical specifications for the *LRS90-3 Laser Radar Scanner* and the *LSS390 Laser Scanner System*. (Courtesy of RIEGL USA.)

Parameter		LRS90-3	LSS390	Units
Maximum range		80	60	m
		262	197	ft
Minimum range		2	1	m
		6.5	3.25	ft
Accuracy		3	10	cm
		1.2	4	ft
Beam divergence		5	3.5	mrad
Sample rate		1000	2000	Hz
Scan range		18	10	$^\circ$
Scan rate		10	10	scans/s
Output	(digital)	RS-232, -422	parallel, RS-422	
Power		11-15	9-16	VDC
		880		mA
Size	(electronics)	22×13×7.6	22×13×7.6	cm
		8.7×5.1×3	8.7×5.1×3	in
	(scanner)	18×10×10	18×10×10	cm
		7×4×4	7×4×4	in
Weight	(electronics)	7.25	2.86	lb
	(scanner)	3.52	2	lb

#### 4.1.2.3 RVSI Long Optical Ranging and Detection System

Robotic Vision Systems, Inc., Hauppauge, NY, has conceptually designed a laser-based TOF ranging system capable of acquiring three-dimensional image data for an entire scene without scanning. The *Long Optical Ranging and Detection System (LORDS)* is a patented concept incorporating an optical encoding technique with ordinary vidicon or solid state camera(s), resulting in precise distance measurement to multiple targets in a scene illuminated by a single laser pulse. The design configuration is relatively simple and comparable in size and weight to traditional TOF and phase-shift measurement laser rangefinders (Figure 4.18).

Major components will include a single laser-energy source; one or more imaging cameras, each with an electronically implemented shuttering mechanism; and the associated control and processing electronics. In a typical configuration, the laser will emit a 25-mJ (millijoule) pulse lasting 1 nanosecond, for an effective transmission of 25 mW. The anticipated operational wavelength will lie between 532 and 830 nanometers, due to the ready availability within this range of the required laser source and imaging arrays.

The cameras will be two-dimensional CCD arrays spaced closely together with parallel optical axes resulting in nearly identical, multiple views of the illuminated surface. Lenses for these cameras will be of the standard photographic varieties between 12 and 135 millimeters. The shuttering

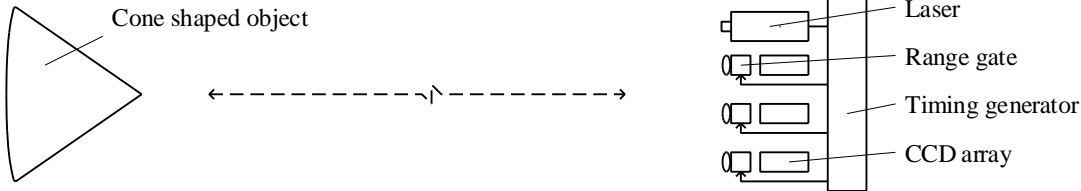


**Figure 4.18:** Simplified block diagram of a three-camera configuration of the LORDS 3-D laser TOF rangefinding system. (Courtesy of Robotics Vision Systems, Inc.)

function will be performed by microchannel plate image intensifiers (MCPs) 18 or 25 millimeters in size, which will be gated in a binary encoding sequence, effectively turning the CCDs on and off during the detection phase. Control of the system will be handled by a single-board processor based on the Motorola *MC-68040*.

*LORDS* obtains three-dimensional image information in real time by employing a novel time-of-flight technique requiring only a single laser pulse to collect all the information for an entire scene. The emitted pulse journeys a finite distance over time; hence, light traveling for 2 milliseconds will illuminate a scene further away than light traveling only 1 millisecond.

The entire sensing range is divided into discrete distance increments, each representing a distinct range plane. This is accomplished by simultaneously gating the MCPs of the observation cameras according to their own unique on-off encoding pattern over the duration of the detection phase. This binary gating alternately blocks and passes any returning reflection of the laser emission off objects within the field-of-view. When the gating cycles of each camera are lined up and compared, there exists a uniquely coded correspondence which can be used to calculate the range to any pixel in the scene.

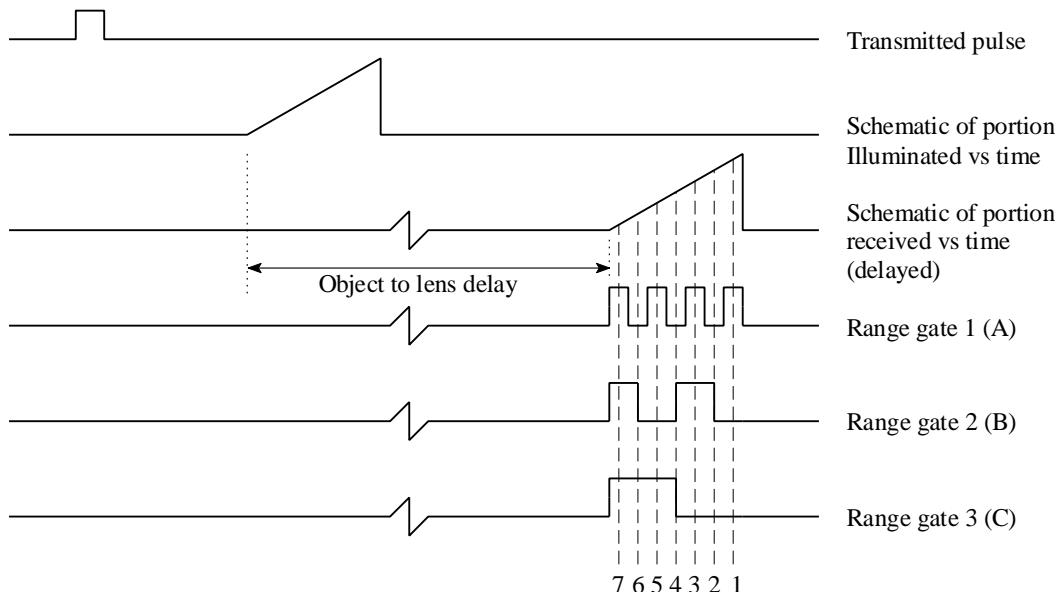


**Figure 4.19:** Range ambiguity is reduced by increasing the number of binary range gates. (Courtesy of Robotic Vision Systems, Inc.)



For instance, in a system configured with only one camera, the gating MCP would be cycled on for half the detection duration, then off the remainder of the time. Figure 4.19 shows any object detected by this camera must be positioned within the first half of the sensor's overall range (half the distance the laser light could travel in the allotted detection time). However, significant distance ambiguity exists because the exact time of detection of the reflected energy could have occurred anywhere within this relatively long interval.

This ambiguity can be reduced by a factor of two through the use of a second camera with its associated gating cycled at twice the rate of the first. This scheme would create two complete *on-off* sequences, one taking place while the first camera is on and the other while the first camera is off. Simple binary logic can be used to combine the camera outputs and further resolve the range. If the first camera did not detect an object but the second did, then by examining the instance when the first camera is off and the second is on, the range to the object can be associated with a relatively specific time frame. Incorporating a third camera at again twice the gating frequency (i.e., two cycles for every one of camera two, and four cycles for every one of camera one) provides even more resolution. As Figure 4.20 shows, for each additional CCD array incorporated into the system, the number of distance divisions is effectively doubled.

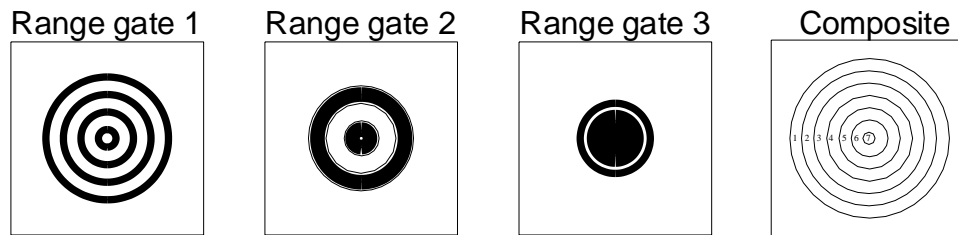


**Figure 4.20:** Binary coded images from range gates 1-3 are combined to generate the composite range map on the far right. (Courtesy of Robotics Vision Systems, Inc.)

Alternatively, the same encoding effect can be achieved using a single camera when little or no relative motion exists between the sensor and the target area. In this scenario, the laser is pulsed multiple times, and the gating frequency for the single camera is sequentially changed at each new transmission. This creates the same detection intervals as before, but with an increase in the time required for data acquisition.

*LORDS* is designed to operate over distances between one meter and several kilometers. An important characteristic is the projected ability to range over selective segments of an observed scene to improve resolution in that the depth of field over which a given number of range increments is spread can be variable. The entire range of interest is initially observed, resulting in the maximum distance between increments (coarse resolution). An object detected at this stage is thus localized to a specific, abbreviated region of the total distance.

The sensor is then electronically reconfigured to cycle only over this region, which significantly shortens the distance between increments, thereby increasing resolution. A known delay is introduced between transmission and the time when the detection/gating process is initiated. The laser light thus travels to the region of interest without concern for objects positioned in the foreground.

## 4.2 Phase-Shift Measurement

The *phase-shift measurement* (or *phase-detection*) ranging technique involves continuous wave transmission as opposed to the short pulsed outputs used in TOF systems. A beam of amplitude-modulated laser, RF, or acoustical energy is directed towards the target. A small portion of this wave (potentially up to six orders of magnitude less in amplitude) is reflected by the object's surface back to the detector along a direct path [Chen et al., 1993]. The returned energy is compared to a simultaneously generated reference that has been split off from the original signal, and the relative phase shift between the two is measured as illustrated in Figure 4.21 to ascertain the round-trip distance the wave has traveled. For high-frequency RF- or laser-based systems, detection is usually preceded by heterodyning the reference and received signals with an intermediate frequency (while preserving the relative phase shift) to allow the phase detector to operate at a more convenient lower frequency [Vuylsteke, 1990].

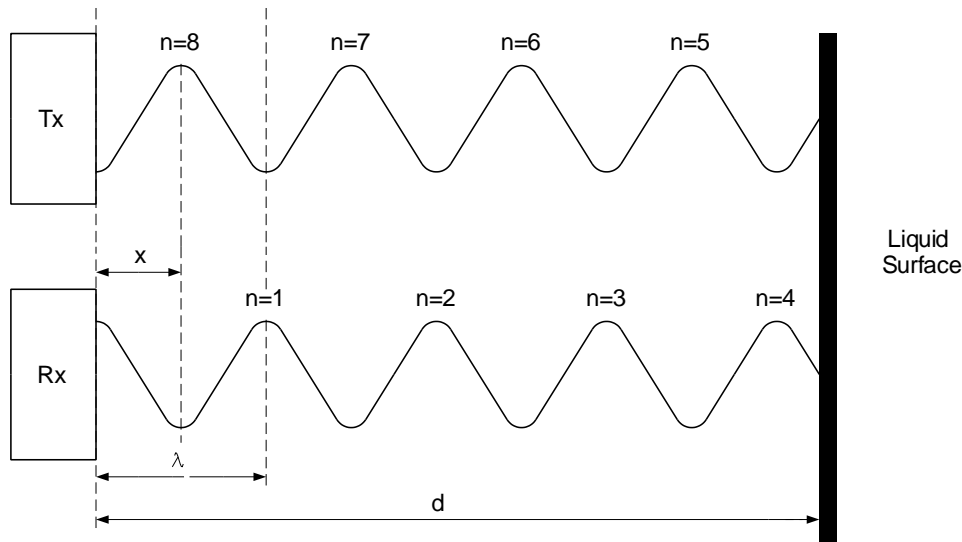


**Figure 4.21:** Relationship between outgoing and reflected waveforms, where  $x$  is the distance corresponding to the differential phase. (Adapted from [Woodbury et al., 1993].)

The relative phase shift expressed as a function of distance to the reflecting target surface is [Woodbury et al., 1993]:

$$\phi = \frac{4\pi d}{\lambda} \quad (4.1)$$

where

$\phi$  = phase shift

$d$  = distance to target

$\lambda$  = modulation wavelength.

The desired distance to target  $d$  as a function of the measured phase shift  $\phi$  is therefore given by

$$d = \frac{\phi\lambda}{4\pi} = \frac{\phi c}{4\pi f} \quad (4.2)$$

where

$f$  = modulation frequency.

For square-wave modulation at the relatively low frequencies typical of ultrasonic systems (20 to 200 kHz), the phase difference between incoming and outgoing waveforms can be measured with the simple linear circuit shown in Figure 4.22 [Figueroa and Barbieri, 1991]. The output of the *exclusive-or* gate goes high whenever its inputs are at opposite logic levels, generating a voltage across capacitor C that is proportional to the phase shift. For example, when the two signals are in phase (i.e.,  $\phi = 0$ ), the gate output stays low and  $V$  is zero; maximum output voltage occurs when  $\phi$  reaches 180 degrees. While easy to implement, this simplistic approach is limited to low frequencies, and may require frequent calibration to compensate for drifts and offsets due to component aging or changes in ambient conditions [Figueroa and Lamancusa, 1992].

At higher frequencies, the phase shift between outgoing and reflected sine waves can be measured by multiplying the two signals together in an electronic mixer, then averaging the product over many modulation cycles [Woodbury et al., 1993]. This integration process can be relatively time consuming, making it difficult to achieve extremely rapid update rates. The result can be expressed mathematically as follows [Woodbury et al., 1993]:

$$\lim_{T \rightarrow \infty} \frac{1}{T} \int_0^T \sin\left(\frac{2\pi c}{\lambda}t + \frac{4\pi d}{\lambda}\right) \sin\left(\frac{2\pi c}{\lambda}t\right) dt \quad (4.3)$$

which reduces to

$$A \cos \frac{4\pi d}{\lambda} \quad (4.4)$$

where

$t$  = time

$T$  = averaging interval

$A$  = amplitude factor from gain of integrating amplifier.

From the earlier expression for  $\phi$ , it can be seen that the quantity actually measured is in fact the *cosine* of the phase shift and not the phase shift itself [Woodbury et al., 1993]. This situation introduces a so-called *ambiguity interval* for scenarios where the round-trip distance exceeds the modulation wavelength (i.e., the phase measurement becomes ambiguous once  $\phi$

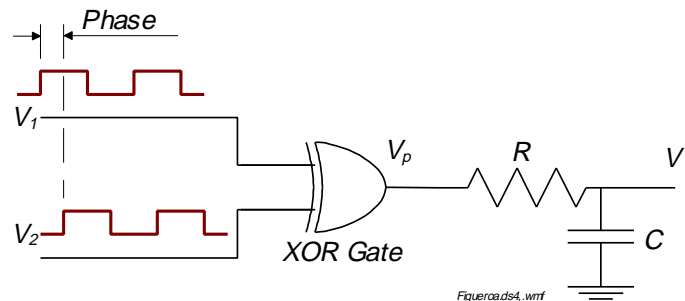


**Figure 4.22:** At low frequencies typical of ultrasonic systems, a simple phase-detection circuit based on an *exclusive-or* gate will generate an analog output voltage proportional to the phase difference seen by the inputs. (Adapted from [Figueroa and Barbieri, 1991].)

exceeds  $360^\circ$ ). Conrad and Sampson [1990] define this ambiguity interval as the maximum range that allows the phase difference to go through one complete cycle of 360 degrees:

$$R_a = \frac{c}{2f} \quad (4.5)$$

where

$R_a$  = ambiguity range interval

$f$  = modulation frequency

$c$  = speed of light.

Referring again to Figure 4.21, it can be seen that the total round-trip distance  $2d$  is equal to some integer number of wavelengths  $n\lambda$  plus the fractional wavelength distance  $x$  associated with the phase shift. Since the cosine relationship is not single valued for all of  $\phi$ , there will be more than one distance  $d$  corresponding to any given phase shift measurement [Woodbury et al., 1993]:

$$\cos\phi = \cos\left(\frac{4\pi d}{\lambda}\right) = \cos\left(\frac{2\pi(x+n\lambda)}{\lambda}\right) \quad (4.6)$$

where:

$d = (x + n\lambda) / 2$  = true distance to target.

$x$  = distance corresponding to differential phase  $\phi$ .

$n$  = number of complete modulation cycles.

The potential for erroneous information as a result of this *ambiguity interval* reduces the appeal of phase-detection schemes. Some applications simply avoid such problems by arranging the optical path so that the maximum possible range is within the ambiguity interval. Alternatively, successive measurements of the same target using two different modulation frequencies can be performed, resulting in two equations with two unknowns, allowing both  $x$  and  $n$  to be uniquely determined. Kerr [1988] describes such an implementation using modulation frequencies of 6 and 32 MHz.

Advantages of continuous-wave systems over pulsed time-of-flight methods include the ability to measure the direction and velocity of a moving target in addition to its range. In 1842, an Austrian by the name of Johann Doppler published a paper describing what has since become known as the *Doppler effect*. This well-known mathematical relationship states that the frequency of an energy wave reflected from an object in motion is a function of the relative velocity between the object and the observer. This subject was discussed in detail in Chapter 1.

As with TOF rangefinders, the paths of the source and the reflected beam are coaxial for phase-shift-measurement systems. This characteristic ensures objects cannot cast shadows when illuminated by the energy source, preventing the *missing parts* problem. Even greater measurement accuracy and overall range can be achieved when cooperative targets are attached to the objects of interest to increase the power density of the return signal.

Laser-based continuous-wave (CW) ranging originated out of work performed at the Stanford Research Institute in the 1970s [Nitzan et al., 1977]. Range accuracies approach those of pulsed laser TOF methods. Only a slight advantage is gained over pulsed TOF ranging, however, since the time-measurement problem is replaced by the need for fairly sophisticated phase-measurement electronics [Depkovich and Wolfe, 1984]. Because of the limited information obtainable from a single range point, laser-based systems are often scanned in one or more directions by either electromechanical or acousto-optical mechanisms.

#### 4.2.1 Odetics Scanning Laser Imaging System

Odetics, Inc., Anaheim, CA, developed an adaptive and versatile scanning laser rangefinder in the early 1980s for use on *ODEX 1*, a six-legged walking robot [Binger and Harris, 1987; Byrd and DeVries, 1990]. The system determines distance by phase-shift measurement, constructing three-dimensional range pictures by panning and tilting the sensor across the field of view. The phase-shift measurement technique was selected over acoustic-ranging, stereo vision and structured light alternatives because of the inherent accuracy and fast update rate.

The imaging system is broken down into the two major subelements depicted in Figure 4.23: the scan unit and the electronics unit. The scan unit houses the laser source, the photodetector, and the scanning mechanism. The laser source is a GaAlAs laser diode emitting at a wavelength of 820 nanometers; the power output is adjustable under software control between 1 to 50 mW. Detection of the returned energy is achieved through use of an avalanche photodiode whose output is routed to the phase-measuring electronics.

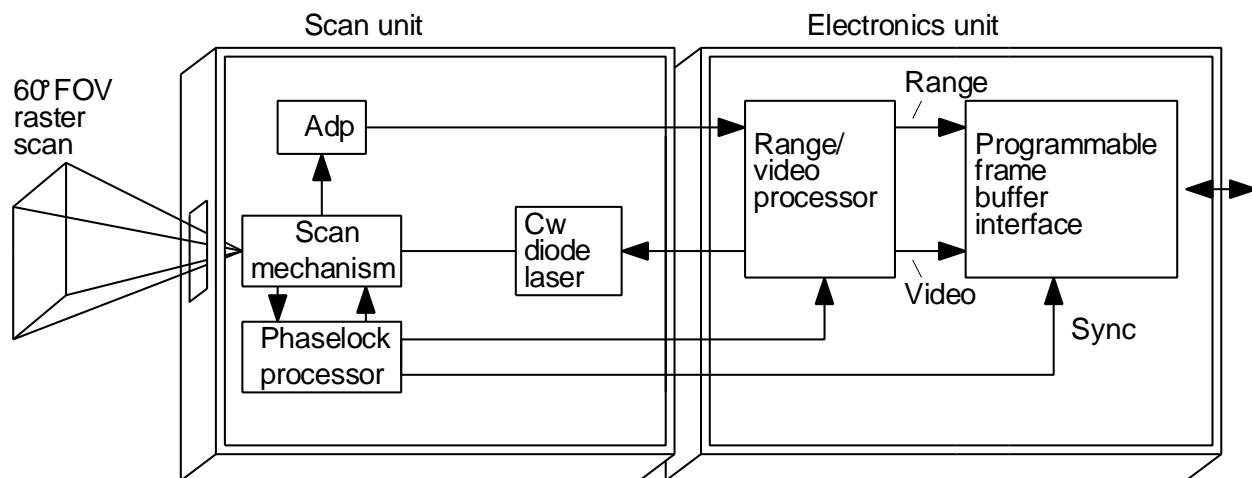


Figure 4.23: Block diagram of the Odetics scanning laser rangefinder. (Courtesy of Odetics, Inc.)

The scanning hardware consists of a rotating polygonal mirror which pans the laser beam across the scene, and a planar mirror whose back-and-forth nodding motion tilts the beam for a realizable field of view of 60 degrees in azimuth and 60 degrees in elevation. The scanning sequence follows a raster-scan pattern and can illuminate and detect an array of  $128 \times 128$  pixels at a frame rate of 1.2 Hz [Boltinghouse et al., 1990].

The second subelement, the electronics unit, contains the range calculating and video processor as well as a programmable frame buffer interface. The range and video processor is responsible for controlling the laser transmission, activation of the scanning mechanism, detection of the returning

energy, and determination of range values. Distance is calculated through a proprietary phase-detection scheme, reported to be fast, fully digital, and self-calibrating with a high signal-to-noise ratio. The minimum observable range is 0.46 meters (1.5 ft), while the maximum range without ambiguity due to phase shifts greater than 360 degrees is 9.3 meters (30 ft).

For each pixel, the processor outputs a range value and a video reflectance value. The video data are equivalent to that obtained from a standard black-and-white television camera, except that interference due to ambient light and shadowing effects are eliminated. The reflectance value is compared to a prespecified threshold to eliminate pixels with insufficient return intensity to be properly processed, thereby eliminating potentially invalid range data; range values are set to maximum for all such pixels [Boltinghouse and Larsen, 1989]. A  $3 \times 3$  *neighborhood median filter* is used to further filter out noise from data qualification, specular reflection, and impulse response [Larson and Boltinghouse, 1988].

The output format is a 16-bit data word consisting of the range value in either 8 or 9 bits, and the video information in either 8 or 7 bits, respectively. The resulting range resolution for the system is 3.66 centimeters (1.44 in) for the 8-bit format, and 1.83 centimeters (0.72 in) with 9 bits. A buffer interface provides interim storage of the data and can execute single-word or whole-block direct-memory-access transfers to external host controllers under program control. Information can also be routed directly to a host without being held in the buffer. Currently, the interface is designed to support *VAX*, *VME-Bus*, *Multibus*, and *IBM-PC/AT* equipment. The scan and electronics unit together weigh 31 lb and require 2 A at 28 VDC.

#### 4.2.2 ESP Optical Ranging System

A low-cost near-infrared rangefinder (see Fig. 4.24, Fig. 4.25, and Tab. 4.10) was developed in 1989 by ESP Technologies, Inc., Lawrenceville, NJ [ESP], for use in autonomous robot cart navigation in factories and similar environments. An eyesafe 2 mW, 820-nanometer LED source is 100 percent modulated at 5 MHz and used to form a collimated 2.5 centimeters (1 in) diameter transmit beam that is unconditionally eye-safe. Reflected radiation is focused by a 10-centimeter (4 in) diameter coaxial Fresnel lens onto the photodetector; the measured phase shift is proportional to the round-trip distance to the illuminated object. The *Optical Ranging System (ORS-1)* provides three outputs: range and angle of the target, and an automatic gain control (AGC) signal [Miller and Wagner, 1987]. Range resolution at 6.1 meters (20 ft) is approximately 6 centimeters (2.5 in), while angular resolution is about 2.5 centimeters (1 in) at a range of 1.5 meters (5 ft).

The *ORS-1* AGC output signal is inversely proportional to the received signal strength and provides information about a target's near-infrared reflectivity, warning against insufficient or excessive signal return [ESP, 1992]. Usable range results are produced only when the corresponding gain signal is within a predetermined operating range. A rotating mirror mounted at 45 degrees to the optical axis provides 360-degree polar-coordinate

**Table 4.10:** Selected specifications for the LED-based near-infrared *Optical Ranging System*. (Courtesy of ESP Technologies, Inc.)

Parameter	Value	Units
Accuracy	< 6	in
AGC output	1-5	V
Output power	2	mW
Beam width	2.5	cm
	1	in
Dimensions	15×15×30	cm
	6×6×12	in
Weight		lb
Power	12	VDC
	2	A

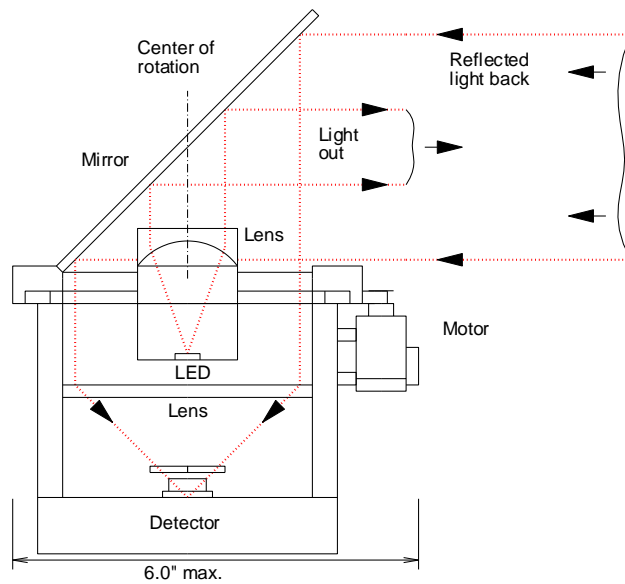


**Figure 4.24:** Schematic drawing of the ORS-1 ranging system. (Courtesy of ESP Technologies, Inc.)

coverage. It is driven at 1 to 2 rps by a motor fitted with an integral incremental encoder and an optical indexing sensor that signals the completion of each revolution. The system is capable of simultaneous operation as a wideband optical communication receiver [Miller and Wagner, 1987].

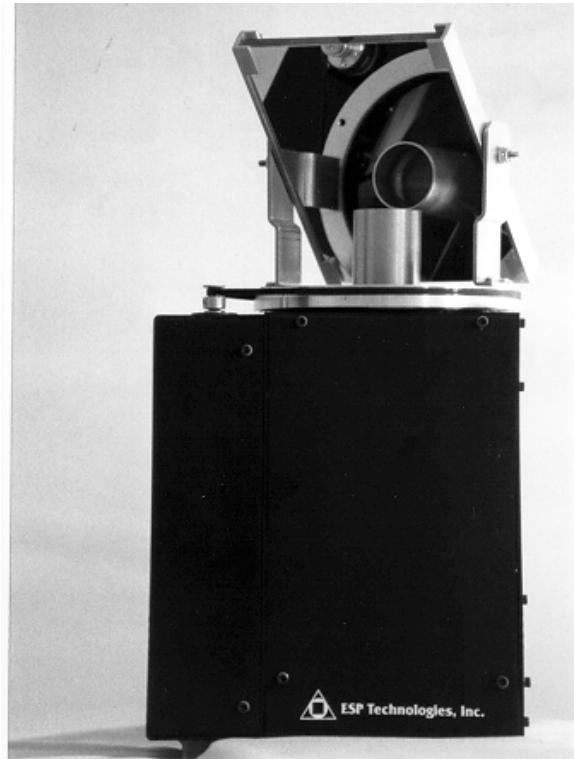


**Figure 4.25:** The ORS-1 ranging system. (Courtesy of ESP Technologies, Inc.)

### 4.2.3 Acuity Research *AccuRange 3000*

Acuity Research, Inc., [ACUITY], Menlo Park, CA, has recently introduced an interesting product capable of acquiring unambiguous range data from 0 to 20 meters (0 to 66 ft) using a proprietary technique similar to conventional phase-shift measurement (see Tab. 4.11). The *AccuRange 3000* (see Figure 4.26) projects a collimated beam of near-infrared or visible laser light, amplitude modulated with a non-sinusoidal waveform at a 50-percent duty cycle. A 63.6-millimeter (2.5 in) collection aperture surrounding the laser diode emitter on the front face of the cylindrical housing gathers any reflected energy returning from the target, and



**Figure 4.26:** The *AccuRange 3000* distance measuring sensor provides a square-wave output that varies inversely in frequency as a function of range. (Courtesy of Acuity Research, Inc.)

compares it to the outgoing reference signal to produce a square-wave output with a period of oscillation proportional to the measured range. The processing electronics reportedly are substantially different, however, from heterodyne phase-detection systems [Clark, 1994].

The frequency of the output signal varies from approximately 50 MHz at zero range to 4 MHz at 20 meters (66 ft). The distance to target can be determined through use of a frequency-to-voltage converter, or by measuring the period with a hardware or software timer [Clark, 1994]. Separate 0 to 10 V analog outputs are provided for returned signal amplitude, ambient light, and temperature to facilitate dynamic calibration for optimal accuracy in demanding applications. The range output changes within 250 nanoseconds to reflect any change in target distance, and all outputs are updated within a worst-case time frame of only 3  $\mu$ s. This rapid response rate (up to 312.5 kHz for all outputs with the optional SCSI interface) allows the beam to be manipulated at a 1,000 to 2,000 Hz rate with the mechanical-scanner option shown in Figure 4.27. A 45-degree balanced-mirror arrangement is rotated under servo-control to deflect the coaxial outgoing and incoming beams for full 360-degree planar coverage.

It is worthwhile noting that the *AccuRange 3000* appears to be quite popular with commercial and academic lidar developers. For example, TRC (see Sec. 4.2.5 and 6.3.5) is using this sensor in their Lidar and Beacon Navigation products, and the University of Kaiserslautern, Germany, (see Sec. 8.2.3) has used the *AccuRange 3000* in their in-house-made lidars.

**Table 4.11:** Selected specifications for the *AccuRange 3000* distance measurement sensor. (Courtesy of Acuity Research, Inc.)

Parameter	Value	Units
Laser output	5	mW
Beam divergence	0.5	mrad
Wavelength	780/670	nm
Maximum range	20	m
	65	ft
Minimum range	0	m
Accuracy	2	mm
Sample rate	up to 312.5	kHz
Response time	3	$\mu$ s
Diameter	7.6	cm
	3	in
Length	14	cm
	5.5	in
Weight	510	g
	18	oz
Power	5 and 12	VDC
	250 and 50	mA



**Figure 4.27:** A 360° beam-deflection capability is provided by an optional single axis rotating scanner. (Courtesy of Acuity Research, Inc.)



#### 4.2.4 TRC Light Direction and Ranging System

Transitions Research Corporation (TRC), Danbury, CT, offers a low-cost *lidar* system (see Figure 4.23) for detecting obstacles in the vicinity of a robot and/or estimating position from local landmarks, based on the previously discussed Acuity Research *AccuRange 3000* unit. TRC adds a 2-DOF scanning mechanism employing a gold front-surfaced mirror specially mounted on a vertical pan axis that rotates between 200 and 900 rpm. The tilt axis of the scanner is mechanically synchronized to nod one complete cycle (down 45° and back to horizontal) per 10 horizontal scans, effectively creating a protective spiral of detection coverage around the robot [TRC, 1994] (see Fig. 4.29). The tilt axis can be mechanically disabled if so desired for 360-degree azimuthal scanning at a fixed elevation angle.

A *68HC11* microprocessor automatically compensates for variations in ambient lighting and sensor temperature, and reports range, bearing, and elevation data via an Ethernet or RS-232 interface. Power requirements are 500 mA at 12 VDC and 100 mA at 5 VDC. Typical operating parameters are listed in Table 4.12.

**Table 4.12:** Selected specifications for the TRC *Light Direction and Ranging System*. (Courtesy of Transitions Research Corp.)

Parameter	Value	Units
Maximum range	12 m 39 ft	
Minimum range	0 m	
Laser output	6 mW	
Wavelength	780 nm	
Beam divergence	0.5 mrad	
Modulation frequency	2 MHz	
Accuracy (range)	25 mm 1 in	
Resolution (range)	5 mm 0.2 in	
(azimuth)	0.18 °	
Sample rate	25 kHz	
Scan rate	200-900 rpm	
Size (scanner)	13×13×35 cm 5×5×13.7 in	
(electronics)	30×26×5 cm 12×10×2 in	
Weight	4.4 lb	
Power	12 and 5 VDC 500 and mA 100	



**Figure 4.28:** The TRC *Light Direction and Ranging System* incorporates a two-axis scanner to provide full-volume coverage sweeping 360° in azimuth and 45° in elevation. (Courtesy of Transitions Research Corp.)

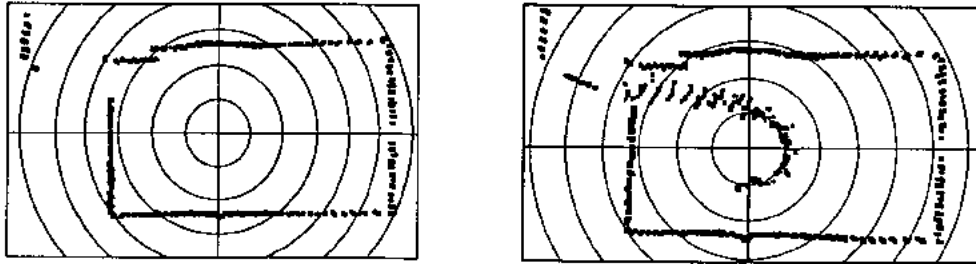


**Figure 4.29:** LightRanger data plotted from scans of a room. An open door at the upper left and a wall in the corridor detected through the open doorway are seen in the image to the left. On the right a trail has been left by a person walking through the room. (Courtesy of Transitions Research Corp.)

#### 4.2.5 Swiss Federal Institute of Technology's “3-D Imaging Scanner”

Researchers at the Swiss Federal Institute of Technology, Zürich, Switzerland, have developed an optical rangefinder designed to overcome many of the problems associated with commercially available optical rangefinders [Adams, 1995]. The design concepts of the *3-D Imaging Scanner* have been derived from Adam's earlier research work at Oxford University, U.K. [Adams, 1992]. Figure 4.30 shows the working prototype of the sensor. The transmitter consists of an eye-safe high-powered (250 mW) Light Emitting Diode (LED) that provides a range resolution of 4.17 cm/° of phase shift between

**Table 4.13:** Preliminary specifications for the *3-D Imaging Scanner*. (Courtesy of [Adams, 1995].)

Parameter	Value	Units
Maximum range	15 m 50 ft	
Minimum range	0 m	
LED power (eye-safe)	1 mW	
Sweep (horizontal)	360 °	
(vertical — “nod”)	130 °	
Resolution (range)	~20 mm 0.8 in	
(azimuth)	0.072 °	
Sample rate	8 kHz	
Size (diameterxheight)	14x27 cm 5.5x10 in	
(electronics)	Not yet determined	
Weight	Not yet determined	
Power	+12 V @ 400 mA -12 V @ 20 mA	

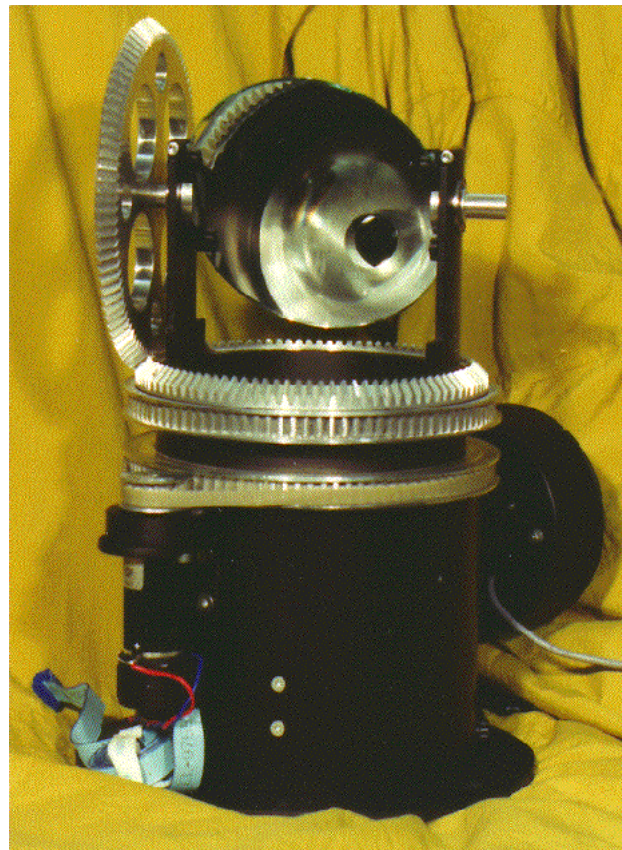


**Figure 4.30:** The *3-D Imaging Scanner* consists of a transmitter which illuminates a target and a receiver to detect the returned light. A range estimate from the sensor to the target is then produced. The mechanism shown sweeps the light beam horizontally and vertically. (Courtesy of [Adams, 1995].)

transmitted and received beams. More detailed specifications are listed in Table 4.13.

The *3-D Imaging Scanner* is now in an advanced prototype stage and the developer plans to market it in the near future [Adams, 1995].

These are some special design features employed in the 3-D Imaging Scanner:

- Each range estimate is accompanied by a range variance estimate, calibrated from the received light intensity. This quantifies the system's confidence in each range data point.
- Direct “crosstalk” has been removed between transmitter and receiver by employing circuit neutralization and correct grounding techniques.
- A software-based discontinuity detector finds spurious points between edges. Such spurious points are caused by the finite optical beamwidth, produced by the sensor's transmitter.
- The newly developed sensor has a tuned load, low-noise, FET input, bipolar amplifier to remove amplitude and ambient light effects.
- Design emphasis on high-frequency issues helps improve the linearity of the amplitude-modulated continuous-wave (phase measuring) sensor.

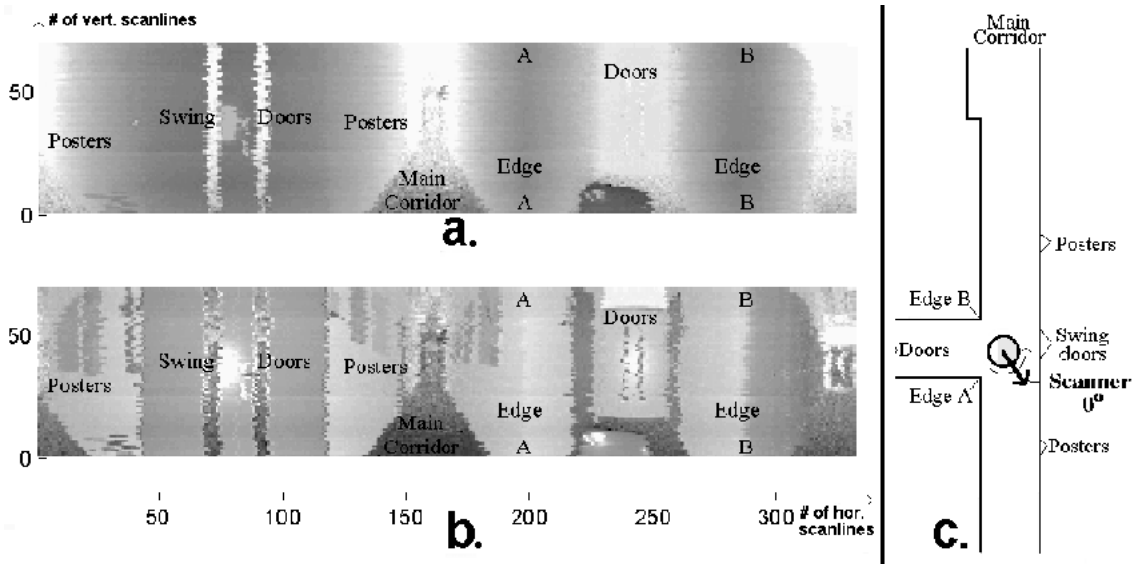
Figure 4.31 shows a typical scan result from the *3-D Imaging Scanner*. The scan is a pixel plot, where the horizontal axis corresponds to the number of samples recorded in a complete 360-degree rotation of the sensor head, and the vertical axis corresponds to the number of 2-dimensional scans recorded. In Figure 4.31 330 readings were recorded per revolution of the sensor mirror in each horizontal plane, and there were 70 complete revolutions of the mirror. The geometry viewed is “wrap-around geometry,” meaning that the vertical pixel set at horizontal coordinate zero is the same as that at horizontal coordinate 330.

#### 4.2.6 Improving Lidar Performance

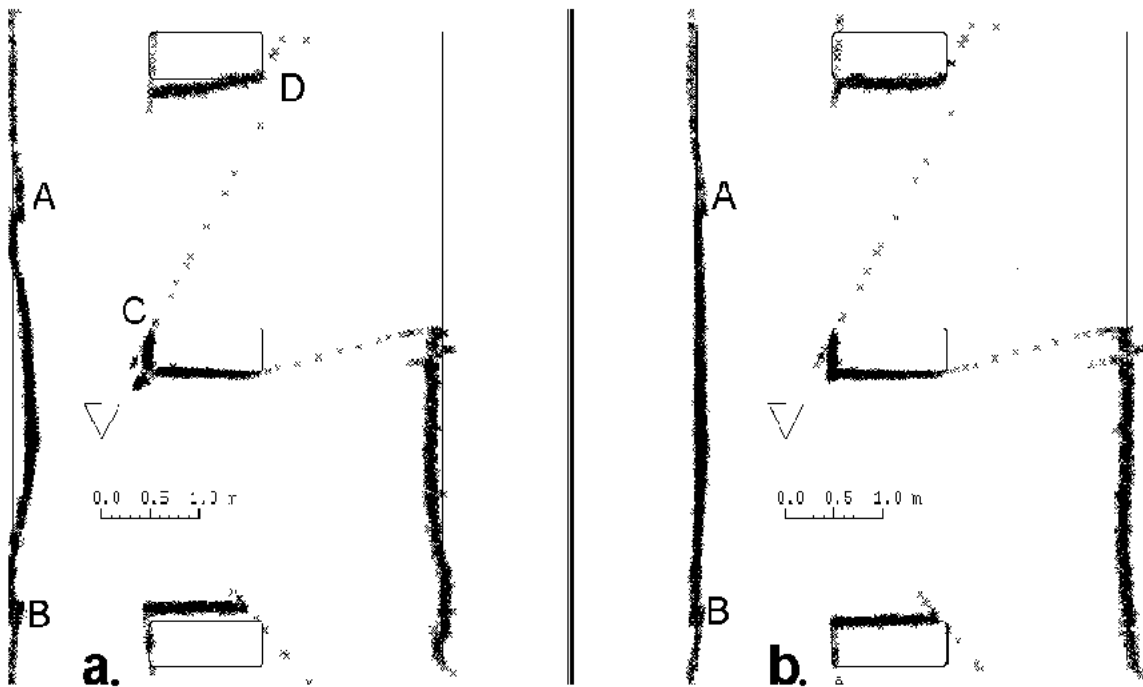
Unpublished results from [Adams, 1995] show that it is possible to further improve the already good performance of lidar systems. For example, in some commercially available sensors the measured phase shift is not only a function of the sensor-to-target range, but also of the received signal amplitude and ambient light conditions [Vestli et al., 1993]. Adams demonstrates this effect in the sample scan shown in Figure 4.32a. This scan was obtained with the ESP *ORS-1* sensor (see Sec. 4.2.3). The solid lines in Figure 4.32 represent the actual environment and each “×” shows a single range data point. The triangle marks the sensor's position in each case. Note the non-linear behavior of the sensor between points A and B.

Figure 4.32b shows the results from the same ESP sensor, but with the receiver unit redesigned and rebuilt by Adams. Specifically, Adams removed the automatic gain controlled circuit, which is largely responsible for the amplitude-induced range error, and replaced it with four soft limiting amplifiers.

This design approximates the behavior of a logarithmic amplifier. As a result, the weak signals are amplified strongly, while stronger signals remain virtually unamplified. The resulting near-linear signal allows for more accurate phase measurements and hence range determination.



**Figure 4.31:** Range and intensity scans obtained with Adams' 3-D Imaging Scanner.  
 a. In the *range scan* the brightness of each pixel is proportional to the range of the signal received (darker pixels are closer).  
 b. In the *intensity scan* the brightness of each pixel is proportional to the amplitude of the signal received.  
 (Courtesy of [Adams, 1995].)



**Figure 4.32:** Scanning results obtained from the ESP ORS-1 lidar. The triangles represent the sensor's position; the lines represent a simple plan view of the environment and each small cross represents a single range data point.  
 a. Some non-linearity can be observed for scans of straight surfaces (e.g., between points A and B).  
 b. Scanning result after applying the signal compression circuit from in [Adams and Probert, 1995].  
 (Reproduced with permission from [Adams and Probert, 1995].)

Note also the spurious data points between edges (e.g., between C and D). These may be attributed to two potential causes:

- The “*ghost-in-the-machine problem*,” in which crosstalk directly between the transmitter and receiver occurs even when no light is returned. Adams' solution involves circuit neutralization and proper grounding procedures.
- The “*beamwidth problem*,” which is caused by the finite transmitted width of the light beam. This problem shows itself in form of range points lying between the edges of two objects located at different distances from the lidar. To overcome this problem Adams designed a software filter capable of finding and rejecting erroneous range readings. Figure 4.33 shows the lidar map after applying the software filter.

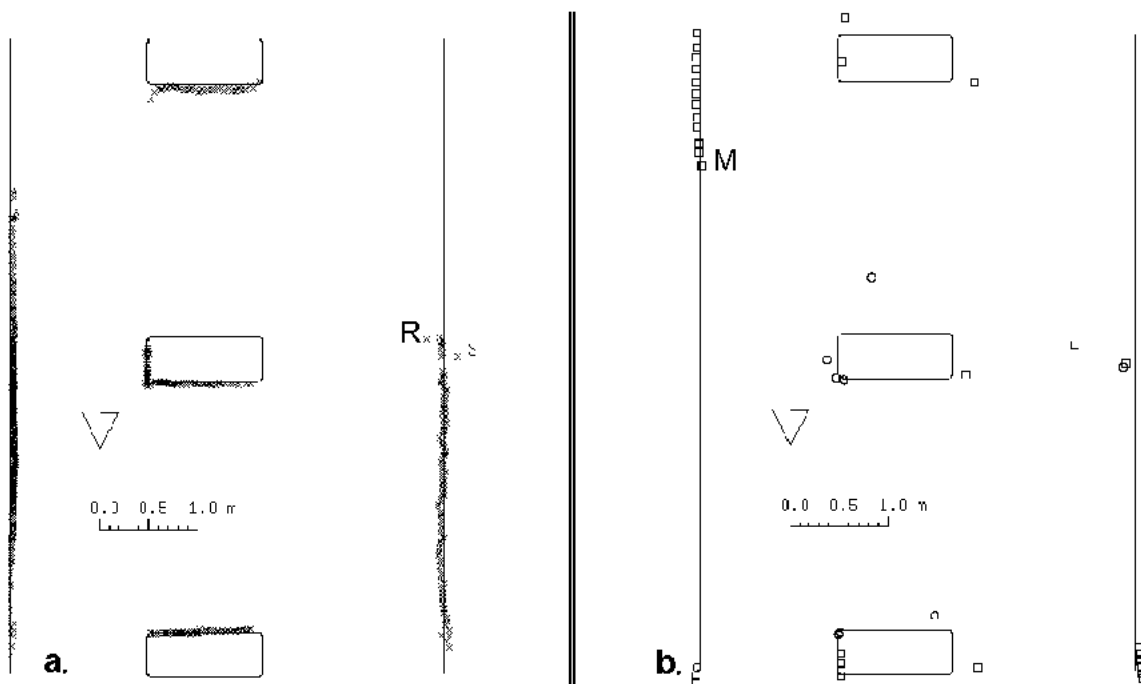


**Figure 4.33:** Resulting lidar map after applying a software filter.

- “Good” data that successfully passed the software filter; R and S are “bad” points that “slipped through.”
- Rejected erroneous data points. Point M (and all other square data points) was rejected because the amplitude of the received signal was too low to pass the filter threshold.

(Reproduced with permission from [Adams and Probert, 1995].)

### 4.3 Frequency Modulation

A closely related alternative to the amplitude-modulated phase-shift-measurement ranging scheme is frequency-modulated (FM) radar. This technique involves transmission of a continuous electromagnetic wave modulated by a periodic triangular signal that adjusts the carrier frequency above and below the mean frequency  $f_0$  as shown in Figure 4.34. The transmitter emits a signal that varies in frequency as a linear function of time:

$$f(t) = f_0 + at \quad (4.7)$$

where

$a$  = constant

$t$  = elapsed time.

This signal is reflected from a target and arrives at the receiver at time  $t + T$ .

$$T = \frac{2d}{c} \quad (4.8)$$

where

$T$  = round-trip propagation time

$d$  = distance to target

$c$  = speed of light.

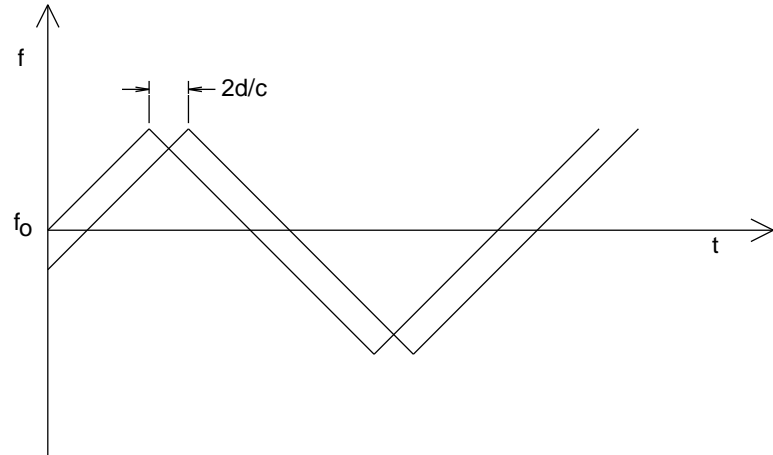


**Figure 4.34:** The received frequency curve is shifted along the time axis relative to the reference frequency [Everett, 1995].

The received signal is compared with a reference signal taken directly from the transmitter. The received frequency curve will be displaced along the time axis relative to the reference frequency curve by an amount equal to the time required for wave propagation to the target and back. (There might also be a vertical displacement of the received waveform along the frequency axis, due to the Doppler effect.) These two frequencies when combined in the mixer produce a beat frequency  $F_b$ :

$$F_b = f(t) - f(T + t) = aT \quad (4.9)$$

where

$a$  = constant.

This beat frequency is measured and used to calculate the distance to the object:

$$d = \frac{F_b c}{4F_r F_d} \quad (4.10)$$

where

$d$  = range to target

$c$  = speed of light

$F_b$  = beat frequency

$F_r$  = repetition (modulation) frequency

$F_d$  = total FM frequency deviation.

Distance measurement is therefore directly proportional to the difference or beat frequency, and as accurate as the linearity of the frequency variation over the counting interval.

Advances in wavelength control of laser diodes now permit this radar ranging technique to be used with lasers. The frequency or wavelength of a laser diode can be shifted by varying its temperature. Consider an example where the wavelength of an 850-nanometer laser diode is shifted by 0.05 nanometers in four seconds: the corresponding frequency shift is 5.17 MHz per nanosecond. This laser beam, when reflected from a surface 1 meter away, would produce a beat frequency of 34.5 MHz. The linearity of the frequency shift controls the accuracy of the system; a frequency linearity of one part in 1000 yards yields an accuracy of 1 millimeter.

The frequency-modulation approach has an advantage over the phase-shift-measurement technique in that a single distance measurement is not ambiguous. (Recall phase-shift systems must perform two or more measurements at different modulation frequencies to be unambiguous.) However, frequency modulation has several disadvantages associated with the required linearity and repeatability of the frequency ramp, as well as the coherence of the laser beam in optical systems. As a consequence, most commercially available FMCW ranging systems are radar-based, while laser devices tend to favor TOF and phase-detection methods.

### 4.3.1 Eaton VORAD Vehicle Detection and Driver Alert System

VORAD Technologies [VORAD-1], in joint venture with [VORAD-2], has developed a commercial millimeter-wave FMCW Doppler radar system designed for use on board a motor vehicle [VORAD-1]. The *Vehicle Collision Warning System* employs a 12.7×12.7-centimeter (5×5 in) antenna/transmitter-receiver package mounted on the front grill of a vehicle to monitor speed of and distance to other traffic or obstacles on the road (see Figure 4.35). The flat etched-array antenna radiates approximately 0.5 mW of power at 24.725 GHz directly down the roadway in a narrow directional beam. A GUNN diode is used for the transmitter, while the receiver employs a balanced-mixer detector [Woll, 1993].

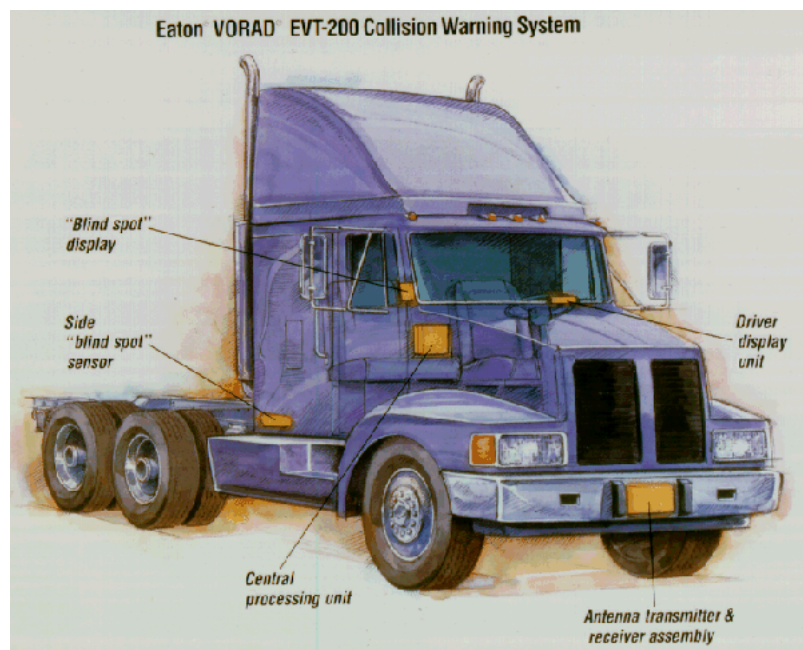


**Figure 4.35:** The forward-looking antenna/transmitter/ receiver module is mounted on the front of the vehicle at a height between 50 and 125 cm, while an optional side antenna can be installed as shown for blind-spot protection. (Courtesy of VORAD-2).

The *Electronics Control Assembly* (see Figure 4.36) located in the passenger compartment or cab can individually distinguish up to 20 moving or stationary objects [Siuru, 1994] out to a maximum range of 106 meters (350 ft); the closest three targets within a prespecified warning distance are tracked at a 30 Hz rate. A Motorola *DSP 56001* and an Intel *87C196* microprocessor calculate range and range-rate information from the RF data and analyze the results in conjunction with vehicle velocity, braking, and steering-angle information. If necessary, the *Control Display Unit* alerts the operator if warranted of potentially hazardous driving situations with a series of caution lights and audible beeps.

As an optional feature, the Vehicle Collision Warning System offers blind-spot detection along the right-hand side of the vehicle out to 4.5 meters (15 ft). The Side Sensor transmitter employs a dielectric resonant oscillator operating in pulsed-Doppler mode at 10.525 GHz, using a flat etched-array antenna with a beamwidth of about 70 degrees [Woll, 1993]. The system microprocessor in the Electronics Control Assembly analyzes the signal strength and frequency components from the Side Sensor subsystem in conjunction with vehicle speed and steering inputs, and activates audible and visual LED alerts if a dangerous condition is thought to exist. (Selected specifications are listed in Tab. 4.14.)

Among other features of interest is a recording feature, which stores 20 minutes of the most recent historical data on a removable EEPROM memory card for post-accident reconstruction. This data includes steering, braking, and idle time. Greyhound Bus Lines recently completed installation of the VORAD radar on all of its 2,400 buses [Bulkeley, 1993], and subsequently reported a 25-year low accident record [Greyhound, 1994]. The entire system weighs just 3 kilograms (6.75 lb), and operates from 12 or 24 VDC with a nominal power consumption of 20 W. An RS-232 digital output is available.

**Table 4.14:** Selected specifications for the Eaton VORAD EVT-200 Collision Warning System. (Courtesy of VORAD-1.)

Parameter	Value	Units
Effective range	0.3-107	m
	1-350	ft
Accuracy	3	%
Update rate	30	Hz
Host platform speed	0.5-120	mph
Closing rate	0.25-100	mph
Operating frequency	24.725	GHz
RF power	0.5	mW
Beamwidth (horizontal)	4	°
	5	°
Size (antenna)	15×20×3	cm
	8	in
	6×8×1.5	
(electronics unit)	20×15×12	cm
	.7	in
	8×6×5	
Weight (total)	6.75	lb
Power	12-24	VDC
	20	W
MTBF	17,000	hr

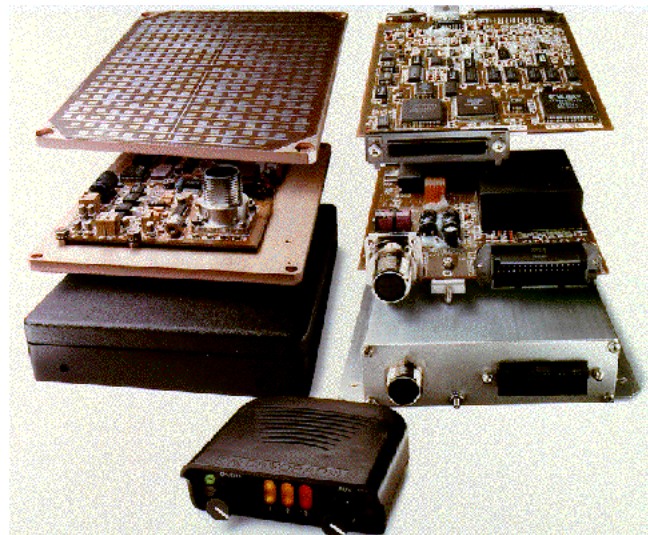


**Figure 4.36:** The electronics control assembly of the Vorad EVT-200 Collision Warning System. (Courtesy of VORAD-2.)



### 4.3.2 Safety First Systems Vehicular Obstacle Detection and Warning System

Safety First Systems, Ltd., Plainview, NY, and General Microwave, Amityville, NY, have teamed to develop and market a 10.525 GHz microwave unit (see Figure 4.37) for use as an automotive blind-spot alert for drivers when backing up or changing lanes [Siuru, 1994]. The narrowband (100-kHz) modified-FMCW technique uses patent-pending phase discrimination augmentation for a 20-fold increase in achievable resolution. For example, a conventional FMCW system operating at 10.525 GHz with a 50 MHz bandwidth is limited to a best-case range resolution of approximately 3 meters (10 ft), while the improved approach can resolve distance to within 18 centimeters (0.6 ft) out to 12 meters (40 ft) [SFS]. Even greater accuracy and maximum ranges (i.e., 48 m — 160 ft) are possible with additional signal processing.

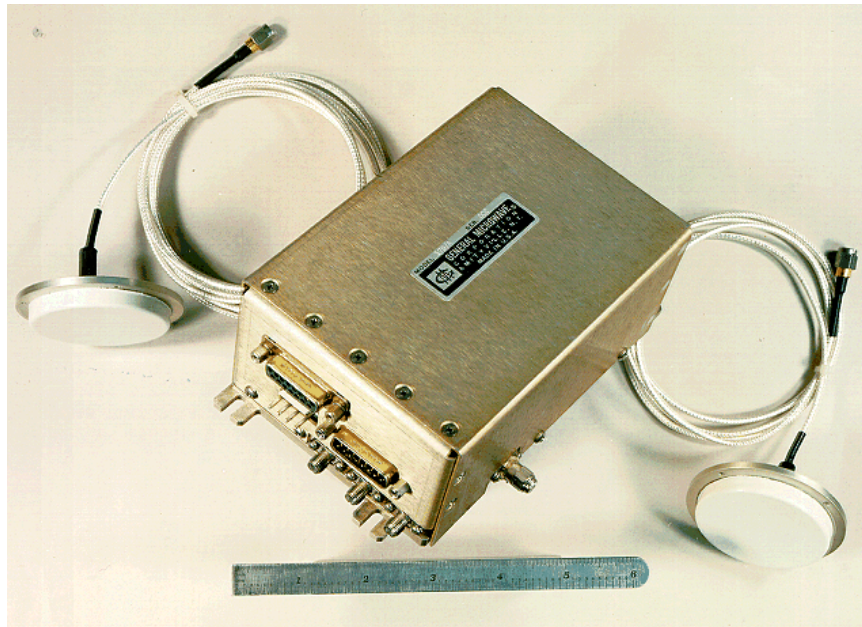


**Figure 4.37:** Safety First/General Microwave Corporation's Collision Avoidance Radar, Model 1707A with two antennas. (Courtesy of Safety First/General Microwave Corp.)

A prototype of the system delivered to Chrysler Corporation uses conformal bistatic microstrip antennae mounted on the rear side panels and rear bumper of a minivan, and can detect both stationary and moving objects within the coverage patterns shown in Figure 4.38. Coarse range information about reflecting targets is represented in four discrete range bins with individual TTL output lines: 0 to 1.83 meters (0 to 6 ft), 1.83 to 3.35 meters (6 to 11 ft), 3.35 to 6.1 meters (11 to 20 ft), and > 6.1 m (20 ft). Average radiated power is about 50  $\mu$ W with a three-percent duty cycle, effectively eliminating adjacent-system interference. The system requires 1.5 A from a single 9 to 18 VDC supply.

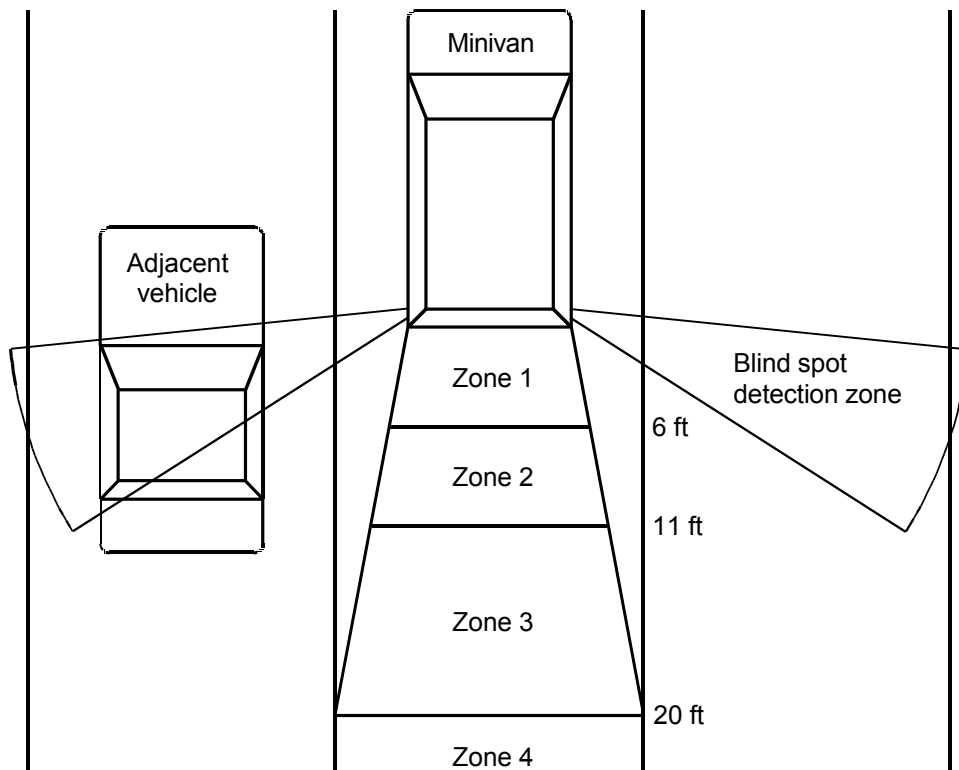


Figure 4.38: The Vehicular Obstacle Detection and Warning System employs a modified FMCW ranging technique for blind-spot detection when backing up or changing lanes. (Courtesy of Safety First Systems, Ltd.)